Pergamon

Geochimica et Cosmochimica Acta, Vol. 65, No. 4, pp. 653–669, 2001

0016-7037/01 $20.00 + .00

PII S0016-7037(00)00555-X

A 35 Myr record of helium in pelagic limestones from Italy: Implications for interplanetary dust accretion from the early Maastrichtian to the middle Eocene

S. MUKHOPADHYAY,[1,*] K. A. FARLEY,[1] and A. MONTANARI[2]

[1]Division of Geological and Planetary Sciences, California Institute of Technology, Pasadena, CA 91125, USA
[2]Osservatorio Geologico di Coldigioco, 62020 Frontale di Apiro, Italy

(*Received May* 30, 2000; *accepted in revised form September* 13, 2000)

Abstract—We have determined the helium concentration and isotopic composition of a suite of early Maastrichtian through middle Eocene pelagic limestones in the Italian Apennines. The results provide a 35 Myr record of the implied flux of extraterrestrial ^{3}He, which is a proxy for the accretion rate of interplanetary dust particles (IDPs).

Our measurements show that the ^{3}He flux was fairly constant in the Maastrichtian, except for possible minor increases (factor of two or less) from ~70.5 Ma to 68 Ma and at ~66 Ma, which probably reflect transient increases in the accretion rate of asteroidal and/or cometary IDPs. We find no evidence for an increase in IDP accretion at or immediately before the K/T boundary, implying that the K/T impact was not associated with enhanced solar system dustiness. This observation precludes the possibility that the K/T impactor was a member of a major comet shower, and is more consistent with impact of a lone comet or asteroid. Our data suggest a 2 to 4 fold increase in IDP accretion between 57 and 54 Ma, followed by a factor of three decrease over an ~4 Myr period in the early to middle Eocene. The duration and magnitude of this variability is inconsistent with previous observations attributed to a shower of long period comets, and is more likely the result of collisions in the asteroid belt/and or Kuiper belt. In the entire 35 Myr record we find no evidence for major enhancements of the IDP accretion rate of the type expected from comet showers. Our results, in combination with earlier ^{3}He measurements, do not support models that predict recurrent comet showers with periods of <38 Myrs. If there is a periodicity in the cratering record that is caused by periodic modulation of the Oort cloud, it is not evident in the Apennine sediment data.

Along with the ^{3}He measurements we also obtained ^{4}He concentrations, which record temporal changes in the flux or composition of terrigenous matter. The most significant change in ^{4}He occurs in the last 4 Myrs of the Cretaceous, over which the concentration of ^{4}He in the detrital component rises by 300%. This rise tracks a strong increase in the seawater ^{87}Sr/^{86}Sr ratio, suggesting a globally significant change in the composition of continental detritus delivered to the oceans, possibly arising from increased continental weathering.

1. INTRODUCTION

Accumulation of interplanetary dust particles (IDPs) enriched in implanted solar wind, solar flare and solar energetic particles (Merrihue, 1964; Ozima et al., 1984; Nier and Schlutter, 1990; Farley, 1995) imparts high helium concentrations and ^{3}He/^{4}He ratios to many deep-sea sediments. Extraterrestrial He is preserved in the sedimentary record for geologically significant periods (Hiyagon, 1994; Farley, 1995) and at least in one instance for 480 Myrs (Patterson et al., 1998). The long-term retention of extraterrestrial He in the sedimentary record provides the potential to characterize the delivery history of IDPs over geologic time (Takayanagi and Ozima, 1987), and several recent studies have investigated this application (Farley, 1995; 1998; Patterson et al., 1998).

IDPs are derived from the asteroid belt, active comets and the Kuiper belt (Nier and Schlutter, 1990; Liou et al., 1996; Flynn, 1999), and presently accrete to the Earth at a rate of about 40×10^6 kg/yr (Love and Brownlee, 1993). These particles range in size from a few μm to a few hundred μm in diameter (Love and Brownlee, 1993), but most IDPs > 35 μm in diameter suffer severe atmospheric heating and He loss (Farley et al., 1997). While occasional large IDPs (50 μm or even larger) collected from the Earth's surface retain some He (Stuart et al., 1999), these particles likely arise from statistically rare conditions such as low entry velocity or angle. Quantitative modeling of entry-heating coupled with observations of seafloor sediments indicates that ^{3}He is predominantly delivered as a surface-correlated component in particles between ~3 and 35 μm diameter (Farley et al., 1997). Like large IDPs, large bodies (>few meters in diameter) are intensely heated and probably vaporized, so they do not contribute substantial amounts of He to the seafloor either. ^{3}He is, therefore, a tracer of only the IDP accretion rate, in contrast to other common extraterrestrial indicators, such as Ir and Os (e.g., Peucker-Ehrenbrink, 1996), which trace the total extraterrestrial mass flux.

Importantly, He accumulating in sediments does not derive from asteroidal, Kuiper-belt, and cometary sources in direct proportion to their abundance in the zodiacal cloud. There is a strong bias toward terrestrial accretion of asteroidal and Kuiper-belt particles over cometary particles, owing to their lower geocentric encounter velocity (Dermott et al., 1996; Kortenkamp and Dermott 1998a; Flynn 1989). Dermott et al. (1996) and Kortenkamp and Dermott (1998a) have argued that a large fraction of IDPs presently accreting to Earth are asteroidal in origin. However, it is likely that the relative propor-

*Author to whom correspondence should be addressed (sujoy@gps.caltech.edu).

tions of asteroidal and cometary IDPs have varied in presently unknown ways over geologic time due to the transient nature of dust sources. The terrestrial accretion rate of IDPs responds rapidly to changing dustiness in the inner solar system because Poynting-Robertson (P-R) drag causes IDPs to be swept into the sun in $\sim 10^4$ to 10^5 years. There are no known mechanisms to buffer the temporal changes in dust production over million year timescales. Therefore, passage of comets or showers of comets into the inner solar system, or major collisions in the asteroid belt or Kuiper belt, are likely to change the total mass accretion and the relative proportions of the IDP components.

^{3}He accumulation in sediments is a sensitive indicator of these phenomena. For example, Farley et al. (1998) reported a long-lived increase in ^{3}He flux in late Eocene sediments containing Ir, shocked quartz, and Ni-rich spinels (Montanari et al., 1993; Clymer et al., 1996; Pierrard et al., 1998), and proposed the occurrence of a shower of long-period comets. Although previously suggested on the basis of orbital dynamics and statistical analysis of the ages of impact craters (Hut et al., 1987), ^{3}He provides the only known record of the enhanced solar system dustiness characteristic of a large comet shower. The geologic history of IDP accretion can therefore provide insights to major events in the solar system and to possible identification of some terrestrial impactors.

To further document variations of solar system dustiness over geologic time and to better characterize the relationship between IDP accretion rate and major terrestrial impacts, especially at the Cretaceous/Tertiary boundary, we undertook a high resolution study (few hundred kyr sampling interval) of the He content and isotopic composition of pelagic limestones ranging from Maastrichtian to middle Eocene in age (74–39 Ma). This study complements the late Eocene record of Farley et al. (1998), and a low resolution ^{3}He study of the entire Cenozoic (Farley, 1995).

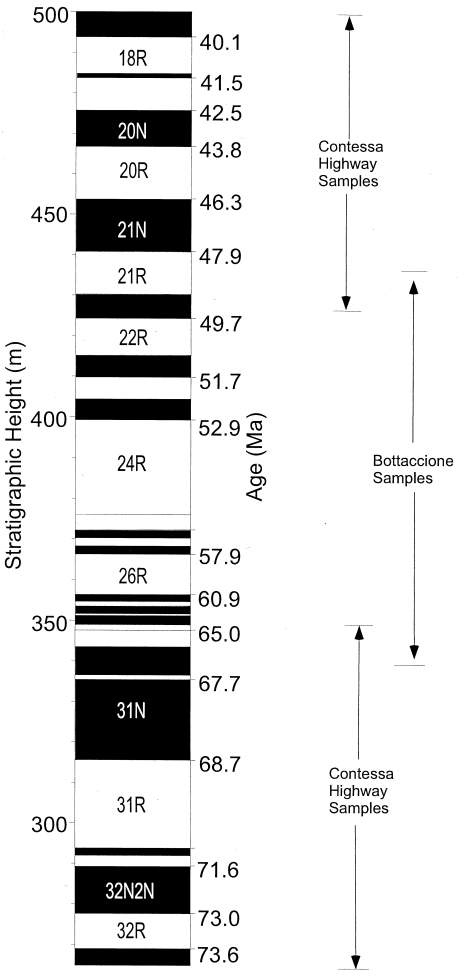

Fig. 1. Composite stratigraphic section based on the correlation between the Contessa and Bottaccione sections (after Alvarez et al., 1977; Napoleone et al., 1983; Chauris et al., 1998). Ages are after Cande and Kent (1995).

2. SAMPLES AND TECHNIQUES

Our samples are part of the Cretaceous to middle Eocene Scaglia Rossa and the middle to late Eocene Scaglia Variegata Formations from the Bottaccione Gorge and Contessa Highway sections at Gubbio, in the Umbrian Apennines of central Italy. The two sections are ~2.5 km apart and have been tightly correlated based on magnetostratigraphy and biostratigraphy (Alvarez et al., 1977; Lowrie and Alvarez, 1977; Roggenthen and Napoleone, 1977; Arthur and Fischer, 1977; Premoli-Silva, 1977; Lowrie et al., 1982; Napoleone et al., 1983; Monechi and Tierstein, 1985; Montanari and Koeberl, 2000). Based on the correlation between the two sections we have constructed a composite stratigraphic section from the early Maastrichtian to the middle Eocene (Fig. 1).

Samples were collected at 1 to 2 m intervals except near the K/T boundary, where they were collected every 0.5 m. The Contessa Highway section was sampled from 73 m below the K/T boundary (early Maastrichtian) to 3 m above the boundary (early Paleocene) and from 79 m to 150 m above the boundary (early to middle Eocene). The Bottaccione Gorge section was sampled from 7 m below the K/T boundary to 90 m above the boundary (the earliest middle Eocene).

Samples were either pulverized with a masonry power drill at the outcrop site, or powdered by hand with a ceramic mortar and pestle in the laboratory. To maximize sample size, aliquots of 2 to 3 g were leached in 10% acetic acid to remove carbonate (Patterson and Farley, 1998), leaving a residue of ~3.3 to 30% of the original samples. Comparison between 2 to 3 g of leached sample and 0.45 g of bulk sediment (Table 1) shows that ^{3}He is not affected by acetic acid leaching, consistent with earlier observations (Patterson and Farley, 1998). Sample preparation, gas extraction, and mass spectrometric techniques are described by Patterson and Farley (1998).

Typical ^{4}He hot blanks were $<0.2 \times 10^{-9}$ cm^3 at standard temperature and pressure (cc STP), and averaged <1% of the ^{4}He in the samples. ^{3}He hot blanks were always $<1 \times 10^{-15}$ cc STP, in all cases < 1% of the sample. The 1σ variation on ~300 standards of similar size to the samples analyzed during this project was 0.5% for ^{4}He and 3.0% for ^{3}He. Note that the natural variability in ^{3}He concentration of a sample (1σ of ~20%) is a much greater source of uncertainty in estimating the extraterrestrial ^{3}He flux than is the analytical precision. We routinely performed repeat extractions and in all cases the amounts of He were at blank levels, indicating complete extraction of He during the initial heating.

Several experiments were undertaken to evaluate possible sources of ^{3}He in addition to that hosted in IDPs. The presence of air-derived ^{3}He was estimated from neon abundance and isotopic ratios from four samples that have He isotopic compositions close to the atmospheric ratio. Gas extraction and purification procedures for Ne were similar to those used for He. Ne was separated from argon in a cryogenic trap held at 78 K and then inlet to the mass spectrometer. All three Ne isotopes were measured on a channeltron multiplier. Ne abundance and isotope ratios were calibrated by comparison to an air standard. The 1σ variation of 4 air standards of similar size to the samples was ~5% for ^{20}Ne, ~5% for ^{20}Ne/^{22}Ne and ~3% for ^{21}Ne/^{22}Ne ratios. Ne measurements were corrected for isobaric interference; the $^{40}Ar^{2+}/^{40}Ar^{+}$ ratio was 0.2 and the CO_2^{2+}/CO_2^{+} ratio was 0.004. The correction to ^{20}Ne

Table 1. Helium concentration in leached and bulk carbonates.

Sample	Type of analyses	No. of analyses	[^{3}He] 10^{-15} cc STP g^{-1} of bulk	[^{4}He] 10^{-9} cc STP g^{-1} of bulk	^{3}He/^{4}He R_A
CON304	Unleached	7	77 ± 28	18.9 ± 4.7	2.91 ± 1.3
CON304	Leached	5	105 ± 9	23.0 ± 0.8	3.68 ± 0.36
CON312	Unleached	20	72 ± 34	41.1 ± 3.9	1.24 ± 0.6
CON312	Leached	4	102 ± 1	30.2 ± 1.1	2.4 ± 0.26

CON refers to samples from the Contessa highway section; errors are 1σ. Note that sample 312 has a higher ^{4}He content in the unleached samples; this could be the result of some ^{4}He in the carbonate material. R_A is the ^{3}He/^{4}He ratio normalized to the atmospheric ratio of 1.39×10^{-6}.

from $^{40}Ar^{2+}$ was <1%, whereas the correction to ^{22}Ne from CO_2^{2+} was negligible.

To determine the contribution of nucleogenic ^{3}He from the ^{6}Li(n,α) reaction we measured the lithium, thorium and uranium concentrations in six samples by inductively coupled plasma mass spectrometry. Aliquots of 2 mg of bulk sediment were taken from the same samples on which He measurements were made. Samples were dissolved in concentrated HF-HNO_3 and spiked with ^{230}Th and ^{235}U for precise determination of U and Th concentrations. Lithium concentrations in the samples were calculated from the Li/^{235}U ratio and by calibrating to a Li standard solution.

3. RESULTS

Helium results for the leached samples are summarized in Table 2. He isotope ratios range from 0.2 to 3.7 times the air ratio (R_A, 1.4×10^{-6}), with a mean of 1.2 R_A. These ratios are elevated with respect to typical crustal values of 0.015 R_A (Tolsthikin 1978; Andrews, 1985), requiring the presence of a high ^{3}He/^{4}He component in the sediments. The likely candidates are cosmogenic, nucleogenic, atmospheric and extraterrestrial He.

3.1. Cosmogenic and Nucleogenic Contributions to ^{3}He

Cosmic ray interactions occurring in the uppermost ~1 m of the Earth's surface produce He with an extremely high ^{3}He/^{4}He ratio (Lal, 1987). Because the limestones we analyzed were deposited in a marine environment, had a long burial history, and were sampled from recently exposed quarry faces or road cuts, postdepositional production of cosmogenic ^{3}He is negligible. While it is possible that the detrital fraction of the sediment was exposed to cosmic rays before deposition, exposure ages of >200 kyrs would be required to account for all of the ^{3}He in our samples using the accepted production rate at sea level and high latitude (Cerling and Craig, 1993). These exposure ages seem unreasonably high, particularly given the fact that detrital minerals have very low He retentivity (Farley, 1995). Low ^{3}He concentrations in loess suggest wind-blown dust contributes negligible amounts of cosmogenic ^{3}He to deep sea sediments (Farley and Patterson, 1995; Farley, in press). We therefore conclude that the limestone samples are unlikely to have significant cosmogenic ^{3}He.

The reaction $^6\text{Li}(n,\alpha) \rightarrow {}^3\text{H} \xrightarrow{\beta} {}^3\text{He}$, is another potential source of ^{3}He in sediments. This reaction yields a correlated production of both He isotopes, with ^{3}He/^{4}He ratios between 0.016 R_A and 0.0016 R_A in typical lithologies (Andrews, 1985). The Li content of the six analyzed Gubbio samples is very low (<7 ppm, Table 3), yielding a calculated ^{3}He/^{4}He production ratio of 0.0014 R_A based on the model of Andrews (1985). This ratio is two to three orders of magnitude lower than the ^{3}He/^{4}He ratios we measure, arguing against significant nucleogenic ^{3}He in our samples. Loosli et al. (1995) and Tolstikhin et al. (1996) called on preferential retention of ^{3}H compared to the α particle to explain their observation of ^{3}He/^{4}He ratios higher than that of nuclear production in some chemical sediments. However, these authors did not consider the presence of an IDP-hosted component, which is almost certainly present, and which we feel is a more likely explanation for their observation.

3.2. Deconvolution of Extraterrestrial and Crustal Helium

In the absence of nucleogenic and cosmogenic components, He in sediments is a mixture of extraterrestrial, crustal, and air-derived He. The relative proportions of these components can be evaluated using He-Ne systematics. Because the He/Ne ratio of the atmosphere is far lower than in extraterrestrial matter (0.3 vs. > 200; Ozima and Pododsek, 1983), the He/Ne ratio of a sediment can be used to identify the presence of atmospheric He (Farley and Patterson, 1995). In 4 limestone samples with ^{3}He/^{4}He ratios close to the atmospheric value, we found He/Ne ratios of >180 (Table 4), implying that less than 1% of the He is air-derived. Therefore, we model the He in our samples as a two-component mixture of extraterrestrial and crustal He. For deconvolution of these two components we assumed that the extraterrestrial endmember has a ^{3}He/^{4}He ratio of 290 R_A, similar to that observed in solar wind and in bulk lunar fines (Geiss et al., 1972; Nier and Schlutter, 1990). For the crustal component we assumed a ^{3}He/^{4}He ratio of 0.03 R_A, similar to that observed in Chinese loess (Farley and Patterson, 1995; Farley, in press). Using these values, the calculated fraction of extraterrestrial ^{3}He in our samples, with the exception of a single sample, is >90%. Even if the ^{3}He/^{4}He ratio of the crustal component were assumed to be 0.15 R_A, well in excess of typical crustal ratios (Andrews, 1985; Farley, in press), the fraction of extraterrestrial ^{3}He would still be dominantly >90% and only in two instances <70%. This difference is much smaller than the inherent variations between samples. Extraterrestrial ^{3}He fluxes computed below are based on this deconvolution, using a crustal ^{3}He/^{4}He ratio of 0.03 R_A.

Deconvolution of the total ^{4}He content yields crustal contri-

Table 2. Average He concentration, ratio, ages, and mass accumulation rates in gubbio carbonates.

Stratigraphic height (m)	^{3}He 10^{-15} cc STP g^{-1}	$\pm 2\sigma$	^{4}He 10^{-9} cc STP g^{-1}	$\pm 2\sigma$	^{3}He/^{4}He R_A	NCF	Age (Ma)	Chron MAR
264.85	40	16	26.0	4.5	1.1	0.06	73.92	3.78
266.00	49	14	24.4	3.0	1.4	0.07	73.83	3.78
267.00	67	27	23.5	4.1	2.0	0.06	73.76	3.78
268.00	38	11	20.8	2.6	1.3	0.05	73.69	3.78
269.00	68	27	20.8	3.6	2.3	0.06	73.62	3.78
270.00	119	33	33.2	4.0	2.7	0.07	73.55	3.78
271.00	23	6	21.7	2.7	0.8	0.06	73.48	3.78
272.00	44	12	30.4	3.7	1.0	0.07	73.40	3.78
273.00	51	14	28.4	3.5	1.3	0.07	73.33	3.78
274.00	49	14	22.3	2.7	1.6	0.06	73.26	3.78
276.00	55	15	19.7	2.4	2.0	0.06	73.12	3.78
277.00	52	14	35.3	4.3	1.1	0.06	73.05	3.78
278.00	76	21	35.6	4.4	1.5	0.09	72.95	2.19
279.00	43	12	27.4	3.4	1.1	0.07	72.83	2.19
280.00	53	9	30.0	2.3	1.3	0.07	72.71	2.19
281.00	49	14	29.9	3.7	1.2	0.07	72.59	2.19
282.00	57	11	27.9	2.2	1.7	0.06	72.46	2.19
283.00	45	13	24.7	3.0	1.3	0.05	72.34	2.19
284.00	67	13	29.3	2.3	1.6	0.06	72.22	2.19
285.00	56	16	25.7	3.1	1.5	0.06	72.09	2.19
286.00	38	9	28.6	2.9	0.9	0.08	71.97	2.19
288.00	25	6	22.8	2.3	0.8	0.06	71.72	2.19
290.00	42	10	21.5	2.2	1.5	0.05	71.51	3.14
291.00	42	10	17.7	1.8	1.7	0.05	71.42	3.14
294.00	45	10	16.2	1.6	2.0	0.04	71.05	2.51
295.35	39	9	20.6	2.1	1.4	0.05	70.90	2.51
298.00	60	24	23.6	2.9	1.9	0.05	70.62	2.51
299.00	42	8	18.1	1.6	1.6	0.03	70.51	2.51
300.00	103	29	27.0	3.3	2.7	0.06	70.40	2.51
301.00	59	16	13.7	1.7	3.1	0.04	70.30	2.51
302.00	51	20	19.4	3.4	1.9	0.06	70.19	2.51
303.00	46	13	20.6	2.5	1.6	0.06	70.08	2.51
304.00	105	19	23.0	1.8	3.7	0.05	69.97	2.51
305.00	49	14	27.0	3.3	1.3	0.05	69.87	2.51
306.00	48	8	22.5	1.5	1.6	0.05	69.76	2.51
307.00	43	12	18.0	2.2	1.7	0.05	69.65	2.51
308.00	53	11	23.3	1.8	1.6	0.05	69.54	2.51
309.00	55	15	19.0	2.3	2.1	0.04	69.44	2.51
310.00	82	23	26.1	3.2	2.2	0.07	69.33	2.51
311.00	46	13	24.2	3.0	1.3	0.05	69.22	2.51
312.00	102	20	30.2	2.1	2.4	0.05	69.11	2.51
313.00	36	10	12.2	1.5	2.1	0.05	69.01	2.51
314.00	44	12	25.8	3.2	1.2	0.06	68.90	2.51
315.00	42	10	20.7	2.1	1.6	0.05	68.79	2.51
316.00	69	19	14.9	1.8	3.3	0.05	68.71	5.39
317.00	77	18	21.6	2.1	2.6	0.06	68.66	5.39
320.00	50	12	17.2	1.7	2.1	0.04	68.51	5.39
323.90	26	6	23.5	2.0	0.8	0.04	68.32	5.39
326.00	45	10	27.7	2.8	1.2	0.06	68.21	5.39
328.00	42	10	26.0	2.6	1.2	0.05	68.11	5.39
330.15	62	12	32.7	2.5	1.4	0.06	68.00	5.39
332.00	29	6	34.0	3.4	0.6	0.05	67.91	5.39
334.00	40	9	61.2	4.8	0.5	0.08	67.81	5.39
336.00	34	8	41.2	4.1	0.6	0.06	67.67	2.16
338.00	29	7	41.4	4.2	0.5	0.06	67.27	0.93
340.00	55	12	41.1	4.1	0.9	0.05	66.69	0.93
340.60	110	44	51.7	8.9	1.5	0.06	66.52	0.93
341.50	99	39	114.4	19.9	0.6	0.09	66.26	0.93
342.00	69	16	62.1	6.2	0.8	0.07	66.11	0.93
342.60	21	8	66.3	11.5	0.2	0.07	65.94	0.93
343.70	159	63	49.5	8.5	2.3	0.05	65.55	1.75
344.00	23	5	43.8	4.4	0.4	0.05	65.50	1.75
344.50	33	13	41.3	7.2	0.6	0.05	65.42	1.75
345.40	43	17	59.4	10.3	0.5	0.07	65.28	1.75
346.00	54	15	46.2	5.7	0.8	0.07	65.19	1.75
346.40	79	31	60.1	10.4	0.9	0.06	65.13	1.75
347.00	39	15	65.1	8.0	0.5	0.07	65.04	1.75

(Continued)

Table 2. (Continued)

Stratigraphic height (m)	^{3}He 10^{-15} cc STP g^{-1}	$\pm 2\sigma$	^{4}He 10^{-9} cc STP g^{-1}	$\pm 2\sigma$	^{3}He/^{4}He R_A	NCF	Age (Ma)	Chron MAR
347.40	23	9	51.8	9.0	0.3	0.05	65.0	1.75
347.80	72	28	37.3	6.5	1.4	0.04	64.91	1.75
348.50	128	50	109.3	19.0	0.8	0.10	64.81	1.75
349.00	114	45	67.7	11.7	1.2	0.10	64.71	0.81
349.50	75	30	49.5	8.6	1.1	0.06	64.54	0.81
349.90	60	24	26.1	4.5	1.6	0.05	64.41	0.81
350.00	72	28	36.9	6.4	1.4	0.07	64.38	0.81
350.50	81	32	55.8	9.7	1.0	0.09	64.21	0.81
351.06	114	45	67.2	11.6	1.2	0.11	64.02	0.81
352.06	160	63	101.7	17.6	1.1	0.12	63.37	0.48
352.71	100	23	60.5	6.1	1.2	0.11	63.00	0.48
353.05	219	50	119.8	12.0	1.3	0.15	62.81	0.48
354.00	148	34	65.0	6.5	1.6	0.10	62.01	0.22
355.00	169	39	88.9	8.9	1.4	0.14	61.20	1.37
356.00	161	64	66.2	11.5	1.7	0.11	61.00	1.37
357.00	167	38	83.9	8.4	1.4	0.12	60.74	0.89
358.00	79	31	37.2	6.4	1.5	0.06	60.43	0.89
359.00	95	22	45.5	4.5	1.5	0.07	60.13	0.89
360.00	109	25	110.7	11.1	0.7	0.10	59.83	0.89
361.00	72	20	52.6	6.5	1.0	0.07	59.52	0.89
362.00	41	9	34.4	3.4	0.9	0.05	59.22	0.89
363.00	58	13	60.2	6.0	0.7	0.08	58.91	0.89
364.00	29	8	35.0	4.3	0.6	0.07	58.61	0.89
365.00	93	26	61.6	7.6	1.1	0.10	58.31	0.89
366.00	53	21	51.6	9.0	0.7	0.09	58.00	0.89
367.00	54	15	58.0	7.1	0.7	0.08	57.79	1.51
368.00	68	19	34.7	4.3	1.3	0.08	57.61	1.51
369.00	120	34	43.9	5.4	2.0	0.09	57.14	0.45
370.00	48	19	34.4	6.0	1.0	0.08	56.54	0.45
371.00	123	34	114.6	14.1	0.8	0.15	56.21	1.10
372.00	102	28	148.8	18.3	0.5	0.22	55.97	1.10
373.00	91	25	104.1	12.8	0.6	0.17	55.82	2.43
375.00	83	23	111.5	13.7	0.5	0.13	55.60	2.43
377.00	110	44	49.9	8.6	1.6	0.08	55.38	2.43
379.00	43	17	19.6	3.4	1.6	0.06	55.15	2.43
381.00	53	21	24.2	4.2	1.6	0.05	54.93	2.43
383.00	59	23	38.0	6.6	1.1	0.08	54.71	2.43
385.00	123	49	62.2	10.8	1.4	0.10	54.49	2.43
387.00	72	28	63.7	11.1	0.8	0.11	54.27	2.43
389.00	51	14	67.5	8.3	0.6	0.12	54.04	2.43
391.00	68	16	37.3	3.7	1.5	0.06	53.82	2.43
393.00	68	15	28.5	2.8	1.7	0.07	53.60	2.43
397.00	89	20	32.2	3.2	2.0	0.06	53.15	2.43
399.00	62	14	27.7	2.8	1.6	0.05	52.93	2.43
401.00	54	15	31.0	3.8	1.3	0.06	52.71	2.50
403.00	56	13	37.9	3.8	1.1	0.08	52.50	2.50
404.90	68	15	60.4	6.1	0.8	0.11	52.29	2.39
405.10	61	14	40.5	4.1	1.0	0.07	52.27	2.39
407.00	51	14	29.1	3.6	1.3	0.06	52.05	2.39
409.00	76	30	68.4	11.9	0.8	0.12	51.83	2.39
411.00	48	19	43.4	7.5	0.8	0.09	51.52	1.54
415.00	100	39	64.2	11.1	1.1	0.11	50.82	1.54
417.00	33	9	41.6	5.1	0.6	0.16	50.57	2.28
419.00	18	5	23.2	2.9	0.6	0.05	50.33	2.28
421.00	29	11	38.9	6.8	0.5	0.06	50.10	2.28
423.00	53	21	32.9	5.7	1.1	0.06	49.86	2.28
425.00	27	11	26.8	4.7	0.7	0.07	49.63	2.39
426.95	51	14	29.9	3.7	1.2	0.07	49.21	2.39
428.54	12	3	21.2	2.6	0.4	0.06	49.23	2.39
429.00	21	8	27.4	4.8	0.6	0.06	49.18	2.39
430.12	32	9	41.5	5.1	0.3	0.09	49.05	2.39
431.00	24	9	37.5	6.5	0.5	0.06	48.96	2.51
432.25	20	5	37.2	4.6	0.4	0.10	48.82	2.51
433.00	46	18	89.5	15.5	0.4	0.07	48.74	2.51
434.98	49	13	61.1	7.5	0.6	0.17	48.53	2.51
435.00	10	4	20.3	3.5	0.4	0.06	48.53	2.51
436.55	33	9	44.3	5.4	0.5	0.08	48.36	2.51

(Continued)

Table 2. (Continued)

Stratigraphic height (m)	^{3}He 10^{-15} cc STP g^{-1}	$\pm 2\sigma$	^{4}He 10^{-9} cc STP g^{-1}	$\pm 2\sigma$	^{3}He/^{4}He R_A	NCF	Age (Ma)	Chron MAR
437.00	28	11	34.3	6.0	0.6	0.06	48.31	2.51
438.65	37	10	35.1	4.3	0.8	0.07	48.13	2.51
440.75	20	5	32.2	4.0	0.4	0.07	47.91	2.51
442.75	35	10	45.8	5.6	0.6	0.12	47.65	2.14
444.75	40	11	39.2	4.8	0.7	0.06	47.40	2.14
446.75	36	10	58.8	7.2	0.4	0.09	47.15	2.14
450.45	41	11	71.6	8.8	0.4	0.11	46.68	2.14
452.75	136	38	132.4	16.3	0.7	0.18	46.39	2.14
454.75	31	8	49.5	6.1	0.5	0.09	46.07	1.42
458.75	46	12	76.0	9.3	0.4	0.11	45.31	1.42
462.60	90	25	95.3	11.7	0.7	0.17	44.58	1.42
464.65	76	21	112.9	13.9	0.5	0.18	44.19	1.42
466.85	30	8	63.0	7.7	0.3	0.13	43.78	1.94
468.95	39	11	77.9	9.6	0.4	0.15	43.48	1.94
473.75	25	7	44.3	5.4	0.4	0.10	42.81	1.94
475.85	41	11	70.0	8.6	0.4	0.12	42.52	2.13
477.75	41	11	65.4	8.0	0.5	0.10	42.28	2.13
479.75	41	11	76.4	9.4	0.4	0.12	42.03	2.13
481.75	41	11	76.3	9.4	0.4	0.13	41.77	2.13
483.75	30	8	47.4	5.8	0.4	0.10	41.52	2.13
486.75	28	11	47.8	5.9	0.4	0.10	41.01	2.16
488.65	23	6	45.3	5.6	0.4	0.11	40.77	2.16
490.75	77	21	103.1	12.7	0.5	0.17	40.51	2.16
492.75	49	13	55.1	6.8	0.6	0.12	40.26	2.16
494.75	170	66	205.2	25.2	0.6	0.31	39.96	1.58
496.75	151	42	138.9	17.0	0.8	0.20	39.62	1.58
497.50	65	18	108.0	13.3	0.4	0.17	39.49	1.58

^{3}He, ^{4}He and ^{3}He/^{4}He represent averages of leached replicates. NCF is the non-carbonate fraction in the sediments as measured by our mass loss data. The age for each sample was calculated from individual chron boundaries assuming a constant sedimentation rate. MAR is the mass accumulation rate in gm/cm^2/kyr calculated from ages of chron boundaries; bulk density of carbonate used = 2.7 gm/cm^3. The position of the K/T boundary is at 347.63 m.

butions >99%, using the same end-members as the previous calculation; no reasonable variations in endmember ratios change the conclusion that ^{4}He is exclusively terrestrial.

3.3. Reproducibility of Replicate Analyses

^{3}He in sediments is carried by a relatively small number of IDP grains that are generally not representatively sampled in 2 to 3 g aliquots (Farley et al., 1997; Patterson and Farley, 1998). This leads to an underestimation of the global mean extraterrestrial ^{3}He flux because rare large particles are under-sampled, and more importantly to a lack of reproducibility in replicate ^{3}He analyses (Farley et al., 1997; Patterson and Farley, 1998). The degree of statistical undersampling depends on the area-time product of the sample, and is 0.125 m^{2}a for our samples, which should undersample the global flux by only ~20% (Farley et al., 1997). Because all of our samples represent approximately the same area-time product (within a factor of a few) this effect can be ignored when considering apparent changes in ^{3}He flux. To reduce the effects of irreproducibility we have replicated measurements on most samples, and on occasions measured a single sample many times.

The reproducibility of these replicate analyses is plotted in Figure 2. The reproducibility distribution is in good agreement with the model prediction of Farley et al. (1997) for sediments with an area-time product of 0.25 m^{2}a, and with the observed distribution from ODP Site 806 (Patterson and Farley, 1998).

Table 3. ^{3}He/^{4}He production ratios.

Stratigraphic height (m)	U ppm	Th ppm	Calculated ^{3}He/^{4}He production ratio (R_A)
279	0.16	0.70	0.0014
299	0.17	0.51	0.0014
314	0.18	0.70	0.0014
326	0.17	0.69	0.0014
334	0.18	0.88	0.0013
341.5	0.19	1.19	0.0013

^{3}He/^{4}He production ratios are calculated using the formulation in Andrews (1985). Neutron capture probabilities used in this calculation are from Andrews and Kay (1982). [Li] in our samples were at blank levels of our acids. (6.8 ppm). We have, therefore, used this value as an upper limit of the [Li] in our samples.

Table 4. He/Ne ratios in selected limestone samples.

Sample	^{3}He/^{4}He R_A	^{4}He conc 10^{-9} cc STP g^{-1}	^{20}Ne conc 10^{-9} cc STP g^{-1}	^{4}He/^{20}He
CON279	1.13	26.4 ± 1.68	0.14 ± .007	195
CON286	1.2	25.8 ± 1.5	0.14 ± .007	181
CON314	0.94	28.6 ± 1.6	0.11 ± .006	256
CON326	1.16	27.7 ± 1.4	0.10 ± .005	284

Limestones were selected with ^{3}He/^{4}He ratios close to the atmospheric ration of 1 R_A. The He/Ne ratio in air is 0.3 and >200 for extraterrestrial matter (Ozima and Podosek, 1983).

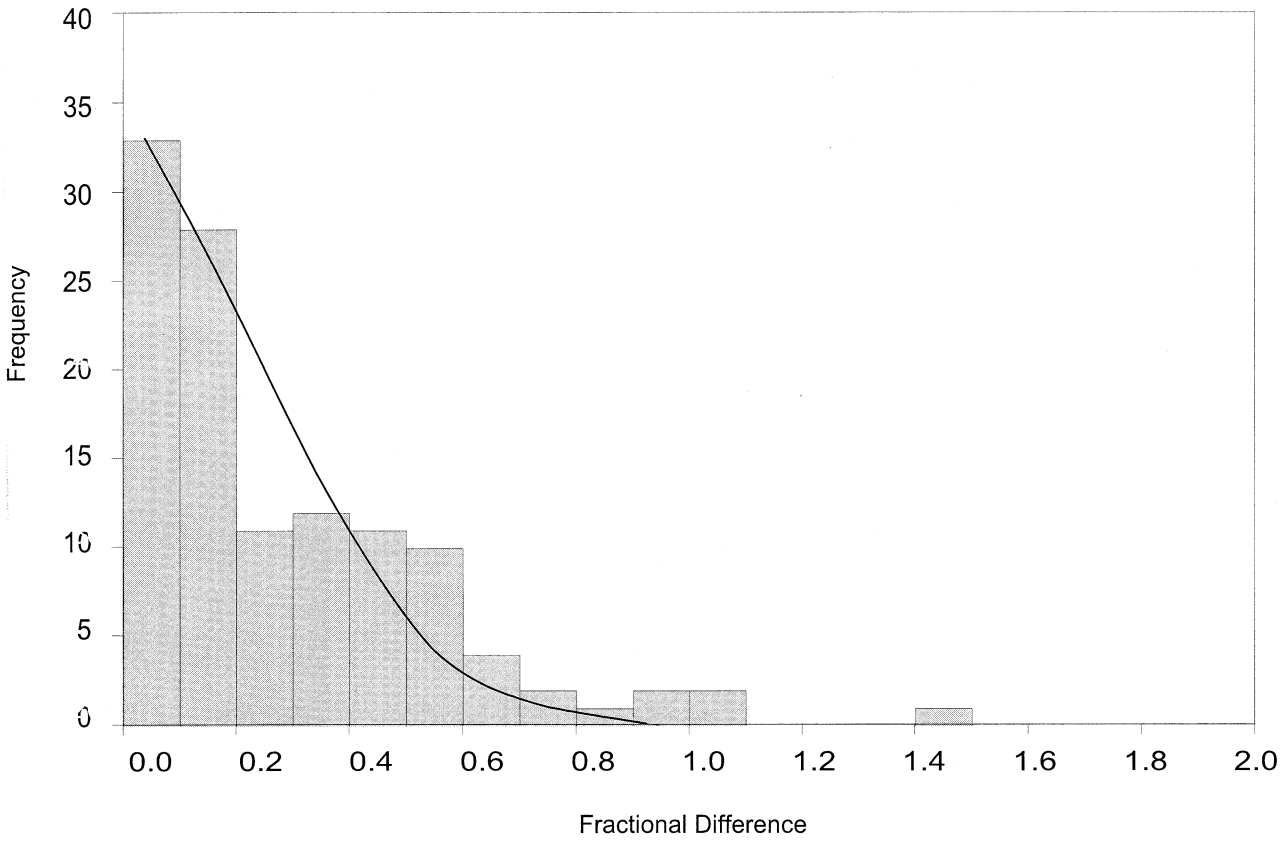

Fig. 2. Observed fractional difference for multiple replicates from the Gubbio sections. Fractional difference is defined as abs[(a1−a2)/(a1+a2)/2], where a1 and a2 represent the replicate analyses of the same sample. For samples that were run more than twice, the fractional difference of the first two analyses is plotted. The solid curve is the distribution modeled for a surface-correlated He component in IDPs subjected to atmospheric entry heating (also see Patterson and Farley, 1998). There is good agreement between the observed and theoretical distributions, and the observed distribution can be approximated by a gaussian with 1σ of ~20%.

Note that while our samples have an area-time product of ~0.125 m^{2}a, a factor of two lower than that used in the model, an order of magnitude difference is required to significantly alter the reproducibility distribution (Farley et al., 1997). The observed distribution can be approximated by a gaussian with 1σ of ~20% (see also Patterson and Farley, 1998). The 2σ uncertainty in our samples, therefore, scales as $40\%/\sqrt{N}$, where N is the number of measurements of a given sample.

In rare cases an individual aliquot of a particular sample may be wildly discrepant compared to replicates. This has been observed previously, and attributed to the presence of rare IDPs with a volume-correlated ^{3}He component (Patterson and Farley. 1998). Using Chauvenet's criterion for elimination of aberrant data points, we have eliminated replicate analyses that plot further than 3σ from the mean of the sample. Fourteen out of 160 replicate analyses were eliminated using this method. Note that the elimination of these points reduces scatter but does not change the overall pattern in Figure 3a.

In contrast to the ^{3}He concentration, the ^{4}He abundances replicate well, with a population standard deviation of 8.7%. This reflects the fact that ^{4}He is derived from terrestrial radiogenic ^{4}He and is sampled fairly representatively in aliquots of 2 to 3 g.

3.4. Helium Concentration and Non-Carbonate Fraction in the Sediments

Figure 3a is a plot of the extraterrestrial ^{3}He concentration ([^{3}He]) as a function of stratigraphic height. There is high frequency scatter in the data; in addition to the statistical effects described above, this scatter may reflect short-term fluctuations in ^{3}He flux or sedimentation rates. Following previous workers (e.g., Farley et al., 1998), to prevent the high frequency variability from obscuring long-term trends, we consider only a five-point running mean through the data. The major features of the smoothed data are:

- [^{3}He] is constant to within a factor of two throughout the Maastrichtian.
- [^{3}He] is low and invariant across the K/T boundary, i.e., from 344.5 (~65.5 Ma) to 348.5 m (~64.8 Ma). This is also seen in a high-resolution study (~20 cm sampling interval) of the K/T boundary from the Bottaccione Gorge section (Mukhopadhyay et al., submitted).
- Starting approximately 2 m above the K/T boundary (349.5 m), [^{3}He] increases and reaches a clear maximum of about four times the Maastrichtian average at 7.5 m above the

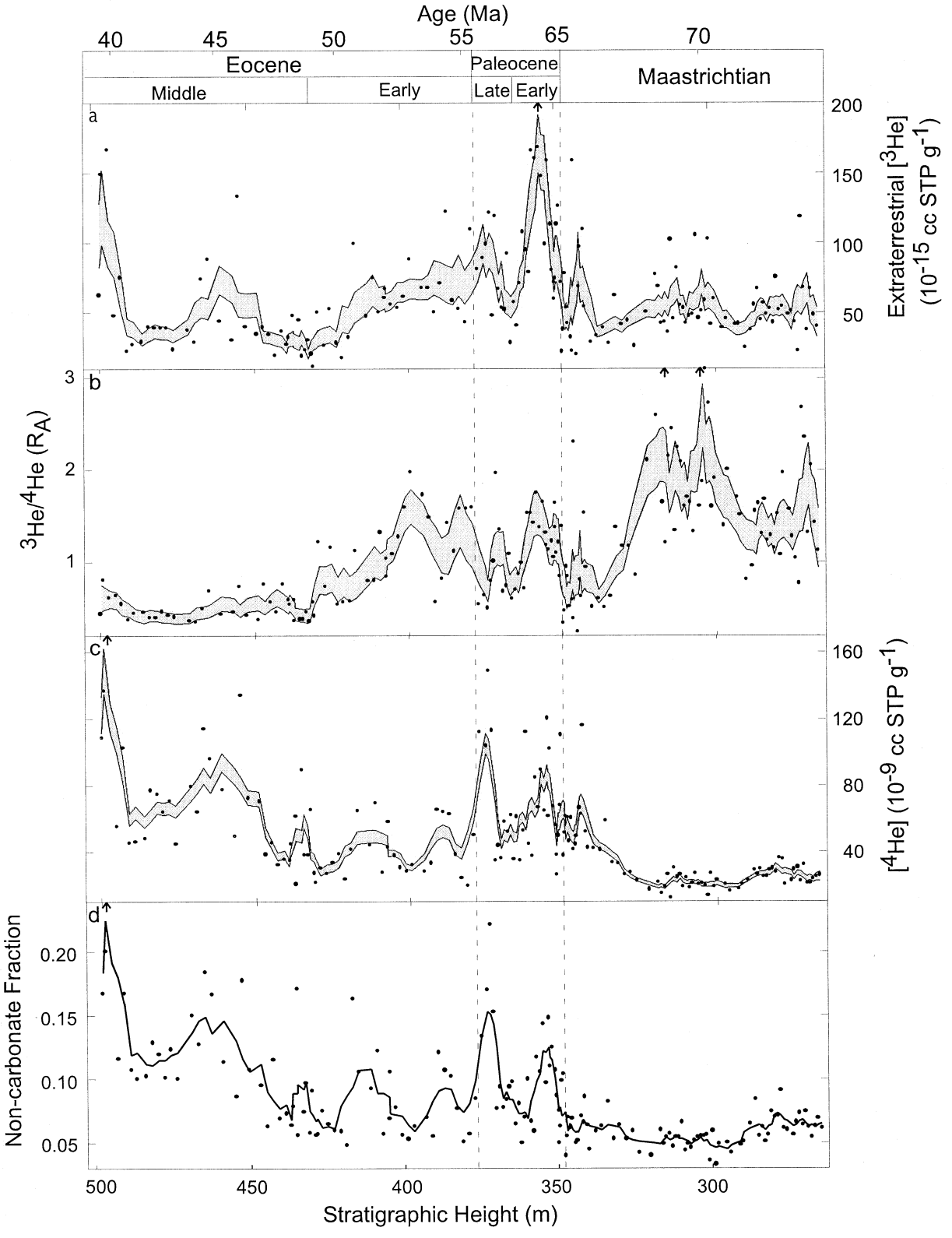

Fig. 3. [^{3}He] (a), ^{3}He/^{4}He ratio (b), [^{4}He] (c), and non-carbonate fraction (d) in the Gubbio sediments. Points are individual values representing the averages of the leached replicates. Arrows represent data points that plot off scale. The shaded envelopes represent the 2σ uncertainty of the five-point running mean calculated from the uncertainties of individual data points. The non-carbonate fraction is operationally defined as the fraction of mass remaining after leaching with acetic acid. The age for each sample was calculated from individual chron boundaries assuming a constant sedimentation rate (solid line in Fig. 4a).

boundary. This is the most prominent feature in the entire 35 Myr record.
- Following a dip in the middle Paleocene, [^{3}He] increases by a factor of two in the late Paleocene, and then steadily declines by a factor of four in the Eocene. The end of the middle Eocene is marked by an increase in [^{3}He].

Figures 3c,d show the crustal ^{4}He concentration ([^{4}He]) and the non-carbonate fraction in the sediments as a function of stratigraphic height. Both of these tracers provide insight to relative sedimentation rates: changes in carbonate sedimentation rate will inversely affect the non-carbonate and ^{4}He contents of the sediment (e.g., Herbert and D'Hondt, 1990; Ten Kate and Sprenger, 1993; Patterson et al., 1999). The major features of these profiles are:

- [^{4}He] and the non-carbonate fraction in the sediments are low and constant through the early Maastrichtian.
- Starting ~27 m below the K/T boundary (320 m), [^{4}He] increases rapidly and monotonically, reaching a maximum of four times early Maastrichtian values at 6 m below the K/T boundary (341.5 m). The non-carbonate fraction in the sediments is, however, approximately constant through this interval.
- Both [^{4}He] and the non-carbonate fraction of the sediments are higher and show more fluctuations in the Eocene when compared to early Maastrichtian values, indicating a higher and variable detrital component during the Eocene (Lowrie et al., 1982).

4. HELIUM FLUX

The extraterrestrial ^{3}He concentration in sediments is controlled by both the ^{3}He flux from space and the sediment mass accumulation rate (MAR) through the relationship [^{3}He] = fR/α, where [^{3}He] is the concentration in sediments, f is the flux of ^{3}He from space, R is the fractional He retentivity (Farley, 1995) and α is the sediment MAR. If the sediment MAR can be determined independently, fR can be calculated. To the extent that R is relatively constant over the interval of interest, the product fR is a proxy for the relative flux of ^{3}He to the seafloor. Because ^{3}He is retained in sediments for hundreds of millions of years (Patterson et al., 1998), assumption of an invariant R over the 35 Myrs of interest here seems appropriate. Here we use the term "implied ^{3}He flux" for the quantity fR derived from a particular sedimentation rate model.

In the absence of absolute and instantaneous sedimentation rates, we have taken two approaches to determining the implied ^{3}He flux. The first is to calculate the average flux for an epoch based on the average sedimentation rate over the epoch. This is a conservative approach because the ages of the epoch boundaries are relatively well known (see Cande and Kent, 1992; Cande and Kent, 1995, and references therein; Gradstein et al., 1994, and references therein), but provides little temporal resolution. The second approach is to calculate the average implied ^{3}He flux over individual magnetochrons based on the average sedimentation rate for the chron. This approach provides about 5× higher temporal resolution but is more uncertain, because the ages of the chron boundaries are often poorly constrained (see Cande and Kent, 1992, and references therein).

The epoch and chron averaged MARs are plotted in Figure 4a. The paleomagnetic data suggest that the MAR in chron 31N (315.5–335.5 m) was more than twice that in chron 31R (293.8–315.5 m). Such a big change in MAR is likely to be controlled by the flux of carbonate, which would change the relative proportions of non-carbonate and carbonate material. However, there is no change in the non-carbonate fraction of the sediments between these chrons (Fig. 3d). Therefore, we speculate that the increase in MAR in chron 31N is not real, but arises from errors in the Cande and Kent (1995) timescale. Below we test this hypothesis using the extraterrestrial [^{3}He] record.

It is also possible that the stratigraphic section was affected by synsedimentary slumps and/or faulting. This leads to uncertainty in the actual stratigraphic thickness of the chron. Evidence for minor synsedimentary slumping and faulting in the Contessa and Bottaccione sections have been presented (Lowrie et al., 1982; Napoleone et al., 1983). The MARs computed for the individual magnetochrons are, therefore, subject to uncertainties that cannot be directly quantified. However, based on our non-carbonate data, the uncertainties in sedimentation rates are unlikely to be greater than a factor of 2 to 3. To identify major extraterrestrial events, we look for large variations in the implied ^{3}He flux that are not correlated with changes in MAR, and which exceed reasonable uncertainties in the MARs.

An alternate and independent approach to determining if variations in [^{3}He] are the result of variations in the ^{3}He accretion rate or are instead the product of sedimentation rate changes is to normalize the [^{3}He] to the non-carbonate fraction ([^{3}He]$_N$) and also to the [^{4}He] in the sediments. As discussed earlier, the non-carbonate fraction and [^{4}He] are crude proxies for the relative sedimentation rate. Therefore, conclusions about changes in ^{3}He accretion rate are most robust when changes in implied ^{3}He flux based on sedimentation rate models are accompanied by changes in [^{3}He]$_N$ and the ^{3}He/^{4}He ratio.

Sedimentary phenomena, such as winnowing or focusing, may cause the computed ^{3}He flux for a given site to differ from the true global flux (Farley and Patterson, 1995; Marcantonio et al., 1996). Extensive discussions on this issue have been presented by Marcantonio et al. (1996), Patterson and Farley (1998), and Farley (in press). In interpreting our results we consider the possibility that focusing might be an issue, and thus have also relied on the [^{3}He] data in conjunction with ^{3}He/^{4}He and [^{3}He]$_N$, neither of which are affected by bulk focusing.

The epoch- and magnetochron-averaged implied ^{3}He flux, and [^{3}He]$_N$, are plotted as a function of age in Figure 4b–d. Our goal is to identify robust features in the He record, and, in the following part of this section, we discuss whether the observed fluctuations in the implied ^{3}He flux are the result of variations in the ^{3}He accretion rate or arise from uncertainties in the calculated MAR.

4.1. Epoch-Averaged Implied ^{3}He Flux

It is evident from Figure 4b that there are no large, long-lived fluctuations in the implied ^{3}He flux. The average implied ^{3}He flux in the Maastrichtian is $135 \pm 5 \times 10^{-15}$ cc STP cm^{-2} kyr^{-1} and is indistinguishable from values in the Oligocene (Farley et al., 1998). The implied ^{3}He flux in the Maastrichtian

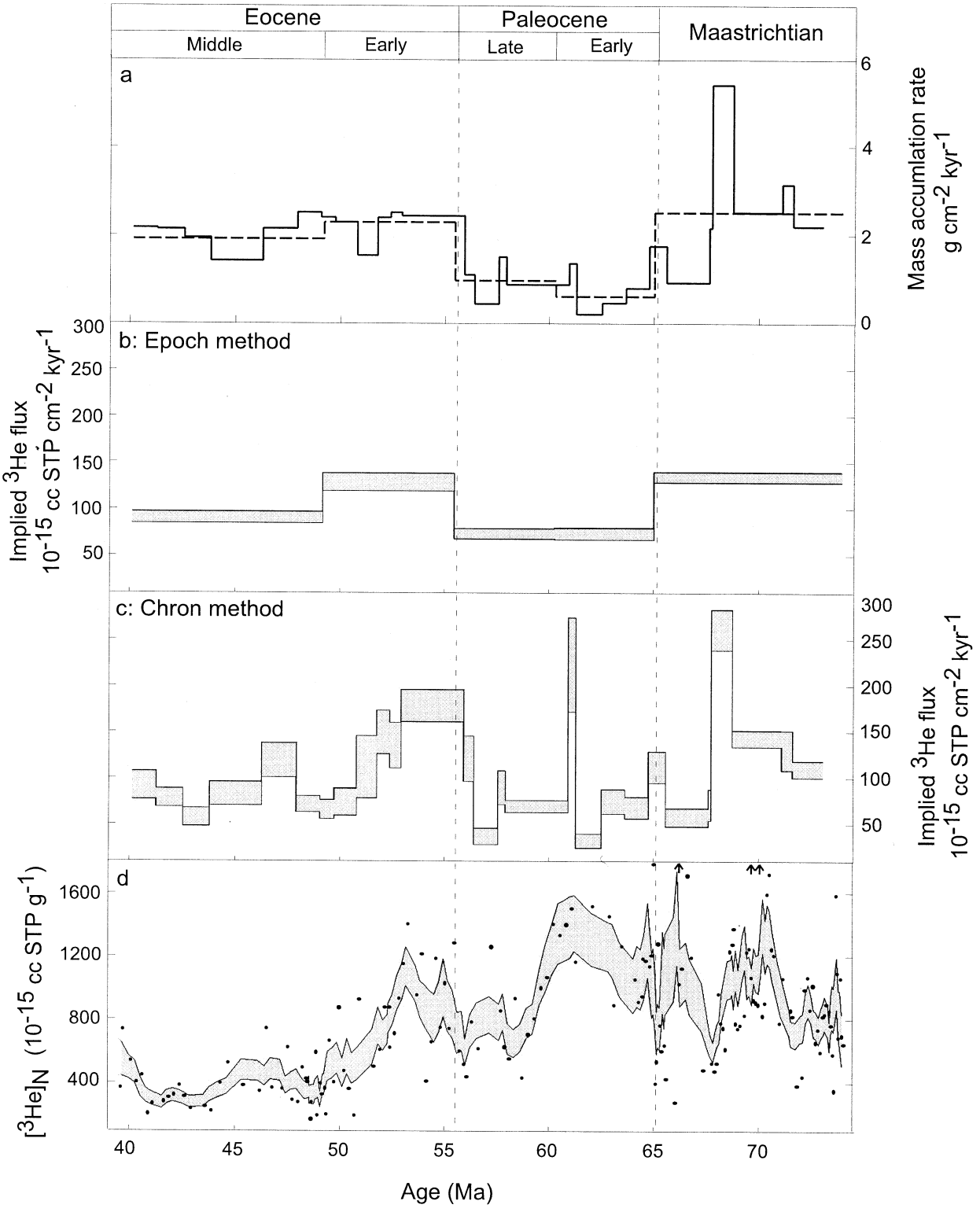

Fig. 4. (a) Sediment mass accumulation rate (MAR) as a function of stratigraphic height. The dashed line is the average MAR in each epoch, while the solid line represents average MAR in individual magnetochrons. (b) Epoch-averaged implied ^{3}He flux. The shaded envelope is the 2σ uncertainty in the implied flux calculated from the 2σ uncertainty in the epoch averaged [^{3}He]. Possible errors in MAR have not been taken into account for calculating the error envelope. (c) Chron-averaged implied ^{3}He flux. Because of incomplete sampling of chrons 32R and 18N, the fluxes for these chrons were not computed. Error envelope calculated as in (b). (d) Non-carbonate normalized [^{3}He]. Points are individual values, and arrows represent data that are off scale. The shaded region is the 2σ uncertainty on the five-point running mean. The age for each sample was calculated as in Figure 3.

and in the early Eocene is almost a factor of two higher than in the entire Paleocene. We note that part of the stratigraphic section is missing in the early Eocene (Napoleone et al., 1983), so the true ^{3}He accretion rate is likely to be higher than our calculated values. These data suggest a factor of two higher extraterrestrial ^{3}He accretion rate during the Maastrichtian and early Eocene when compared to the Paleocene.

4.2. Chron-Averaged Implied ^{3}He Flux

4.2.1. Maastrichtian

The most prominent feature in the Maastrichtian record is the factor of ~2.5 enhancement occurring between 68.7 Ma and 67.7 Ma, in chron 31N. However, this peak does not arise from higher [^{3}He] but from a short-term increase in MAR (Fig. 4a). In addition, [^{3}He], ^{3}He/^{4}He ratio, and $[^3He]_N$ actually decrease between 68.7 and 67.7 Ma (Fig. 3a,b and 4d). These observations are inconsistent with a rise in the ^{3}He accretion rate. Instead, as noted earlier, we believe that there is an error in the calculated MAR resulting from an error in the Cande and Kent (1995) timescale. Assuming that the average implied ^{3}He flux in the Maastrichtian holds for this chron, we calculate a duration of 2 Myr for chron 31N, instead of the1 Myr interval suggested by Cande and Kent (1995). This increase would bring the sediment MAR in to good agreement with the surrounding section (Fig. 4a).

In contrast to the chron 31N peak, there are minor synchronous elevations (factor of two) in $[^3He]_N$, ^{3}He/^{4}He ratio and [^{3}He] at ~70.5 Ma and ~66 Ma. These observations suggest minor increases (~ factor of two) in the extraterrestrial ^{3}He accretion rate between 70.5 and 68 Ma and at ~66 Ma.

4.2.2. K/T boundary

The implied ^{3}He flux across the K/T boundary, between 65.5 Ma and 64.8 Ma, is $\sim 120 \times 10^{-15}$ cc STP cm^{-2} kyr^{-1}, slightly lower that the Maastrichtian average (Fig. 4b,c). Along with [^{3}He], ^{3}He/^{4}He ratio, and $[^3He]_N$, the implied flux suggests a low and near constant extraterrestrial ^{3}He accretion rate at the K/T boundary. This result is corroborated by a high-resolution study of the boundary interval (Mukhopadhyay et al., submitted). There is a fourfold increase in the [^{3}He] concentration 2 m above the K/T boundary, but the implied ^{3}He flux remains nearly constant at 75×10^{-15} cc STP cm^{-2} kyr^{-1} in the early Paleocene. The increase in [^{3}He], therefore, reflects a decrease in the sedimentation rate (further considered by Mukhopadhyay et al., submitted).

4.2.3. Paleocene

The implied ^{3}He flux is nearly constant in the Paleocene, except for a spike at ~61 Ma (Fig. 4c), in chron 27N. However, this increase correlates with a short-lived, sixfold increase in the MAR, and is not associated with a sharp increase in [^{3}He], ^{3}He/^{4}He ratio, or $[^3He]_N$. We conclude that the increase in implied ^{3}He flux at ~61 Ma is due to an error in the MAR. Taking the average implied ^{3}He flux of $\sim 75 \times 10^{-15}$ cc STP cm^{-2} kyr^{-1} for the Paleocene implies a duration of ~1 Myr for chron 27 N instead of the 356 kyr suggested by the Cande and Kent (1995) timescale. We conclude that the extraterrestrial ^{3}He accretion rate in the Paleocene was essentially invariant

4.2.4. Paleocene/Eocene

Between ~57 Ma and 54 Ma the chron averaged implied ^{3}He flux increases by a factor of 4.5 over the late Paleocene values (Fig. 4c), an increase which is correlated with a 2.5-fold enhancement in [^{3}He] between 57 and 56 Ma (Fig. 3a). The ^{3}He/^{4}He ratio and $[^3He]_N$ are approximately constant between 57 and 56 Ma, but increase by a factor of two in the interval from 56 to 54 Ma (Fig. 3b and 4d). Unfortunately there are several factors that complicate interpretation of the peak in implied flux. First, marly layers in the late Paleocene/early Eocene sediments imply rapid but poorly constrained variations in MAR. These variations in MAR could reflect either primary biogenic productivity (R. Coccioni, private communication) or short-term fluctuations in the terrigenous flux. Note that an enhancement in the terrigenous flux, between 57 and 56 Ma, would suppress a rise in the ^{3}He/^{4}He ratio and $[^3He]_N$, and may explain the difference in timing of the increases in extraterrestrial [^{3}He], ^{3}He/^{4}He ratio and $[^3He]_N$. Second, Napoleone et al. (1983) report tectonic disturbances, such as faulting and synsedimentary slumping, in this part of the stratigraphic section, and suggest that part of chron 24R is missing at Bottaccione.

Despite these factors, the data suggest a two to fourfold enhancement in extraterrestrial ^{3}He accretion between ~56 Ma and 54 Ma, the exact timing and magnitude of which are equivocal. We suggest that this increase should be verified from a stratigraphic section free of tectonic disturbance and/or facies changes. Note that if part of the stratigraphic section is missing (as implied by the work of Napoleone et al., 1983), the calculated MAR is less than the true value. Therefore the suggested increase is a lower limit to the true magnitude of the increase in extraterrestrial ^{3}He accretion.

4.2.5. Eocene

While the magnitude and timing of the increase in extraterrestrial ^{3}He accretion at the P/E boundary or in the early Eocene is debatable, the data strongly suggest that the extraterrestrial ^{3}He accretion rate decreased by a factor of three between 54 and ~50 Ma (Fig. 4c). The decrease in implied ^{3}He flux is mirrored by similar decreases in [^{3}He], ^{3}He/^{4}He ratio, and $[^3He]_N$, so it is not likely to be a sedimentation phenomenon. The alternative possibility of a three fold decrease in the MAR is inconsistent with the paleomagnetic data, and our non-carbonate and ^{4}He data (Fig. 3c,d and 4a; see also Lowrie et al., 1982; Napoleone et al., 1983). Therefore it seems necessary to conclude that the extraterrestrial ^{3}He accretion rate decreased by a factor of three in the early Eocene over a period of 4 to 5 Myrs.

Although there is an increase in [^{3}He] at the end of the middle Eocene in chron 18N, we cannot evaluate this part of the record since the magnetochron continues beyond the currently accessible part of the stratigraphic section.

5. DISCUSSION

Helium analyses in the Gubbio limestones provide information on the flux of ^{3}He and ^{4}He to the seafloor over a 35 Myr

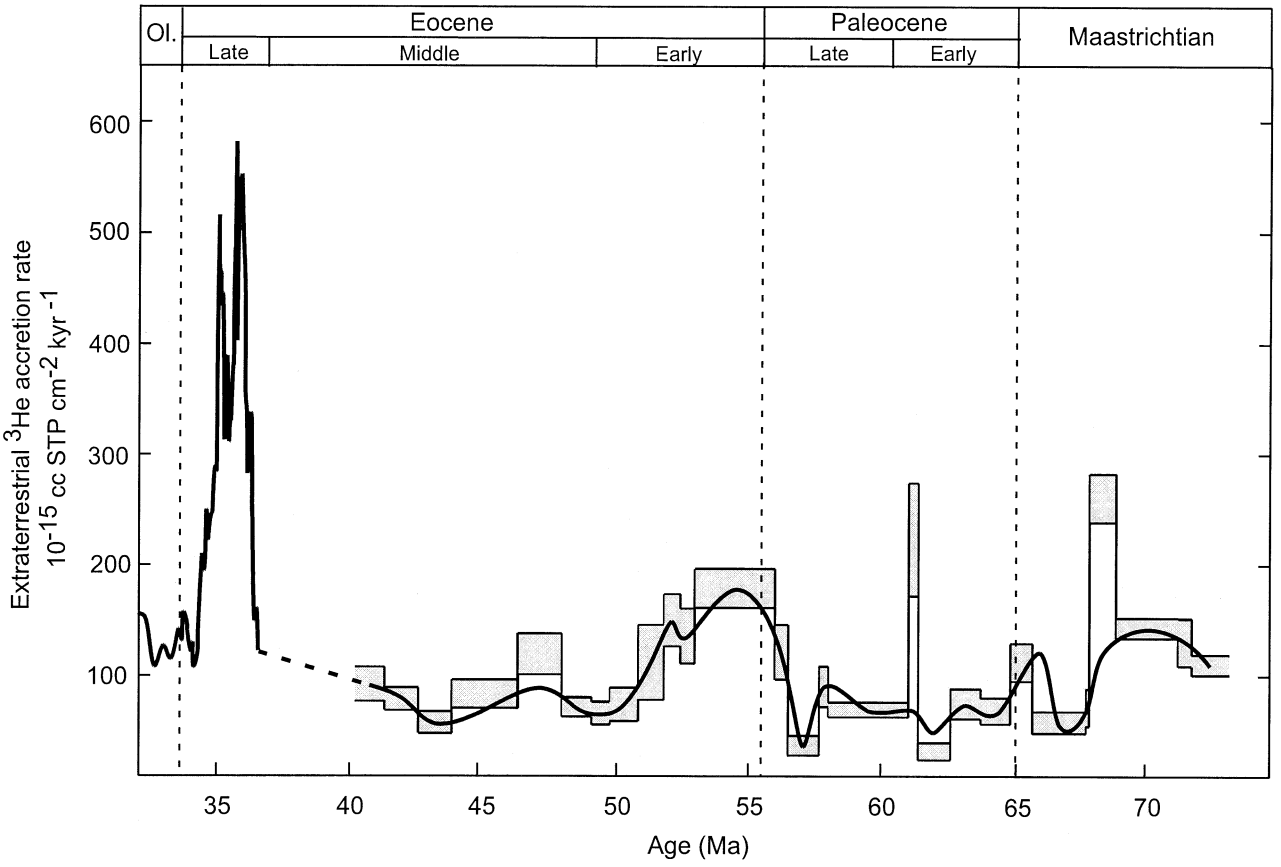

Fig. 5. Extraterrestrial ^{3}He accretion rate. The solid line represents our best estimate of the extraterrestrial ^{3}He accretion rate from 74 to 39 Ma, based on the arguments presented in the text. The late Eocene data is from Farley et al. (1998). The dotted line is an interpolation of the extraterrestrial ^{3}He flux between 39 and 36 Ma. The shaded envelope is the same as in Figure 4c.

period from the Maastrichtian to the middle Eocene. These two isotopes are almost completely independent of each other, with ^{3}He overwhelmingly derived from interplanetary dust, and ^{4}He from terrigenous matter. Here we discuss the implications of the record of these two tracers.

5.1. IDP Accretion

Based on the arguments in the previous section, our best estimate of the ^{3}He accretion rate from the Apennine sections is presented in Figure 5. The shape of the ^{3}He profile is generally similar to the low temporal resolution record from a pelagic clay core in the central Pacific (LL44-GPC3; Farley, 1995), but the implied fluxes at Gubbio are on average a factor of four lower. The origin of this discrepancy is not yet known. The area-time products of the samples composing these two records are similar, so differential undersampling is unlikely to be the cause. However it is possible that diagenetic effects are involved. For example, Patterson et al. (1998) found that the magnetic fraction in subaerially exposed 480 Myr old marine limestone carried no measurable ^{3}He, in contrast to pelagic clays from the GPC3 core, where the magnetic fraction carries $>$50% of the total ^{3}He (Farley 1995; in press). It is possible that extended subaerial exposure leads to decomposition of ^{3}He-bearing magnetic grains, leaving only a second, more resistant carrier. More work is required to address the issue, e.g., by determining the carrier phase(s) responsible for long term retention of ^{3}He. Regardless of this discrepancy, the similarity of pattern between the high-resolution Gubbio record and that from GPC3 gives us confidence that our record provides a global, but relative, history of the terrestrial ^{3}He accretion rate.

The ^{3}He record from Gubbio is most simply interpreted in terms of variations in the terrestrial accretion rate of IDPs arising from various solar system processes, a hypothesis supported by the correlation of terrestrial impacts with a several Myr period of enhanced ^{3}He accretion in the late Eocene (Farley et al., 1998). Although other processes may affect the ^{3}He accretion rate (e.g., changes in solar wind output), we believe these processes are less significant than those that directly modulate the abundance of IDPs in the zodiacal cloud (also see Farley, in press). Here we consider processes responsible for the pattern shown in Figure 5, and how variations in IDP accretion may be related to terrestrial impact events.

Cometary particles are an important component of the zodiacal cloud (Liou et al., 1995). While a single comet is unlikely to substantially modify dust abundances or terrestrial impact probability, the abundance of active comets can be tremen-

dously enhanced over a two to several million-year period by gravitational perturbation of the Oort cloud (e.g., Hills, 1981; Byl, 1983; Heisler and Tremaine, 1986; Matese et al., 1995). Such an event is expected to increase the IDP accretion rate and the probability of terrestrial impacts over the duration of the shower. Although comet showers have been invoked to explain various aspects of the terrestrial cratering record, beside the late Eocene event (Farley et al., 1998) little observational evidence exists regarding the timing and recurrence interval of these important events.

Major collisions in the asteroid belt are also expected to increase the abundance of IDPs in the zodiacal cloud. Depending on grain size, dust from the asteroid belt becomes earth crossing in $\sim 10^4$ to 10^5 years after collision due to P-R drag. Larger bodies ejected from the asteroid belt by the collision can become Earth-crossing on time scales in excess of 1 Myr and possibly as long as 100 Myr, if they do so at all (Gladman, 1997). Therefore, a close ($\sim 10^6$ years) temporal correlation between IDP accretion rates and impacts following a major collision in the asteroid belt is not expected a priori (also see Kortenkamp and Dermott, 1998b; Farley, in press). This distinction provides one approach by which to distinguish enhanced IDP accretion from a comet shower vs. that from an asteroidal collision.

A third possible mechanism for increasing the IDP accretion is associated with major collisions in the Kuiper belt. Dust production in the Kuiper belt may significantly exceed that in the asteroid belt (Flynn, 1999). Liou et al. (1996) suggested that ~20% of the dust produced by the Kuiper belt enters the inner solar system, but dust grains bigger than 9 μm will probably be destroyed by collisions with interstellar grains. However, particles < 9 μm may be recorded by ^{3}He in sediments. Further work is needed to establish the timescale of enhanced dustiness and its relationship to terrestrial impact following a collision between Kuiper belt objects.

Our data preclude large, long-lived variations in ^{3}He accretion rate (Fig. 4b). However, factor of 2 to 4 variations in the ^{3}He accretion rate are suggested. Below we discuss possible origins of these fluctuations; the relation, if any, between this record and known terrestrial impacts; and the implications of our data for models predicting periodic showers of long-period comets.

Minor increases (<factor of 2) in the extraterrestrial ^{3}He accretion rate are suggested between 70.5 and 68 Ma and at ~66 Ma, 1 Myr before the K/T boundary. These peaks are at the margin of detection, far smaller and of shorter duration than the late Eocene peak (Fig. 5). Two moderately large impact craters of Maastrichtian age are known: Manson (37 km diameter, 74.1 ± 0.1 Ma, Izett et al., 1998) and Kara Ust-Kara (70.3 ± 2.2 Ma, Trieloff et al., 1998). Kara Ust-Kara is either a single crater or two different craters, and diameter estimates are between 70 and 120 km for the two structures (Koeberl et al., 1990, Nazarov et al., 1991). While Manson is older than the increase in ^{3}He accretion, the age of Kara Ust-Kara overlaps with the peak at 70.5 Ma. A high-resolution iridium (Ir) profile down to 305 m in the Bottaccione section, corresponding to ~71 Ma, failed to reveal any anomalies in the Ir abundance (Alvarez et al., 1990). Therefore, the minor peaks in ^{3}He accretion rate seen in the Maastrichtian are not in any clear way correlated with impact indicators. If these peaks are real, they probably reflect minor fluctuations in the dustiness of the inner solar system associated with random events in the asteroid and/or Kuiper belt.

The nature of the K/T impactor is a matter of debate upon which our observations have bearing. Suggested candidates include member(s) of a comet shower (e.g., Hut et al., 1987) or an asteroid/comet with a carbonaceous chondritic composition (e.g., Shukolyukov and Lugmair, 1998; Kyte, 1998). Based on data from the GPC3 core, Farley (1995) argued against substantial enhancement in the ^{3}He accretion rate at the K/T boundary. Similarly, our Gubbio analyses reveal a low and constant extraterrestrial ^{3}He accretion rate between 66 Ma and ~57 Ma, implying a low and invariant solar system IDP abundance through this time interval. This observation argues strongly against the possibility that the K/T bolide was associated with a comet shower. Instead our results support the hypothesis that a single earth-crossing asteroid or comet was responsible for the K/T impact. Further consideration of the K/T impact is presented elsewhere (Mukhopadhyay et al., submitted).

Our data suggest a two to fourfold increase in ^{3}He accretion rate near the P/E boundary (~55 Ma), followed by a decrease over an ~4 to 5 Myr period. A ^{3}He peak at about this time was also found in the GPC3 core (Farley, 1995). The GPC3 peak appears to be of longer duration, but may be smeared by bioturbation. The P/E peak at Gubbio is similar in shape to the far larger ^{3}He peak observed in the late Eocene, previously attributed to a shower of long-period comets (Fig. 5 and Farley et al., 1998). Like the late Eocene peak, the P/E peak is asymmetric, with the rise occurring faster than the decline, but is of substantially longer duration than found in the late Eocene. Modeling suggests that comet showers generated by close stellar encounters decay with a period of only 1 to 2 Myr (Hut et al., 1987; Weissman, 1982). The decrease in IDP accretion from 54 to 50 Ma occurs over a longer period, arguing against a comet shower produced by an impulsive perturbation of the Oort cloud. Alternatively, it has been proposed that perturbation of the Oort cloud by Galactic tidal forces may cause a broad maximum in the comet flux over a several million year period with a peak-to-trough comet flux variation of 4:1 (Matese et al., 1995). However, the flux of these long-period comets is predicted to rise and fall symmetrically. This contrasts with the strongly asymmetric P/E peak we have identified. Thus we are aware of no cometary mechanism which predicts a peak of the type we observe.

There are three moderately large impact craters in the Paleocene/early Eocene: Montagnais (D = 45 km; age = 50.5 ± 0.8 Ma; Bottomley and York, 1988), Kamensk (D = 25 km; Age = 49.2 ± 0.2 Ma; Izett et al., 1994) and Marquez Dome (D = 13 km; Age = 58.3 ± 3.1; Sharpton and Gibson, 1990; McHone and Sorkhabi, 1994). With the possible exception of Marquez Dome, these impacts are not temporally correlated with the P/E peak. No correlated PGE anomalies were reported from pelagic clay cores in the Pacific, despite measurements covering this period (Kyte and Wasson, 1986; Peucker-Ehrenbrink, 1996). Although Schmitz et al. (1997) reported a small Ir anomaly in the latest Paleocene, no shocked quartz was found, leaving the origin of the Ir enrichment uncertain. Thus, we find no clear evidence for impact features that correlate with the P/E peak, further distinguishing it from the late Eocene peak.

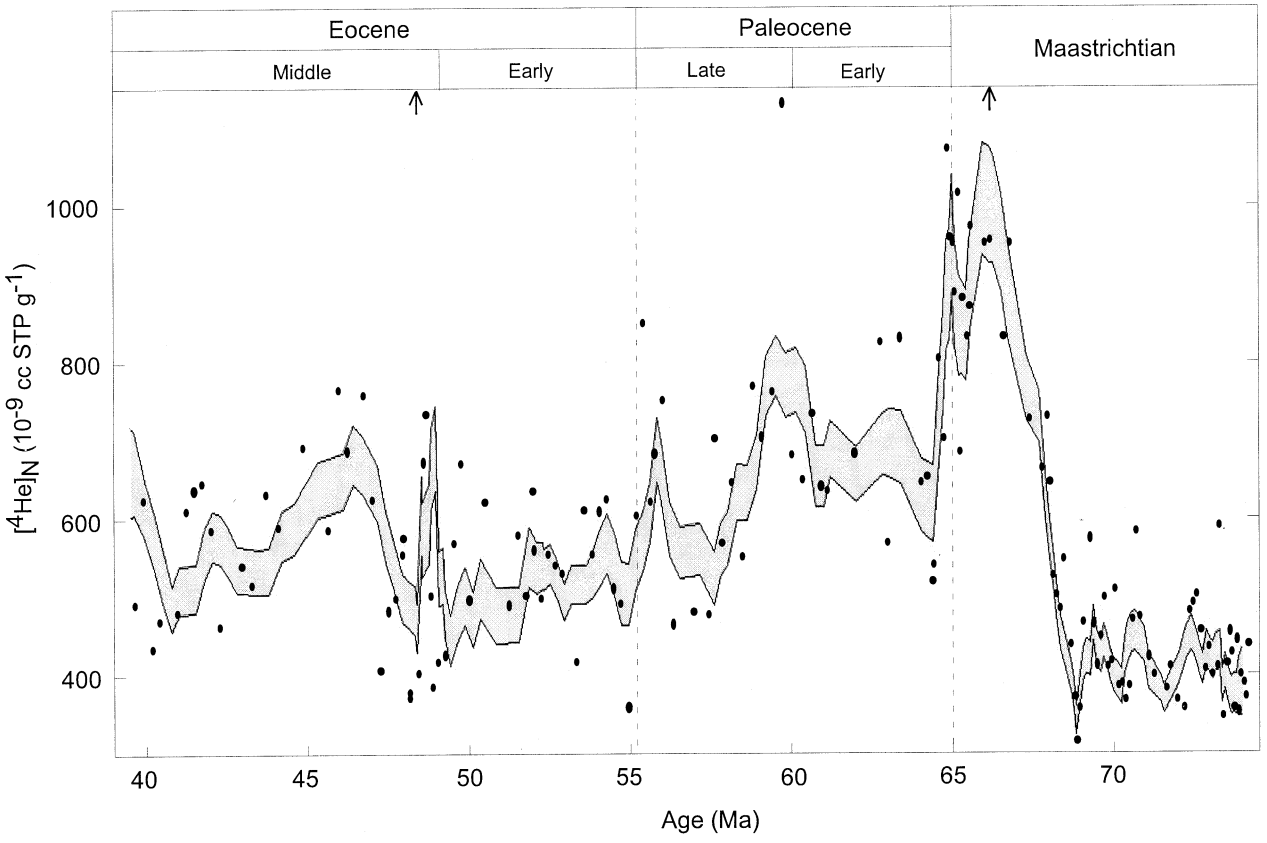

Fig. 6. $[^4He]_N$ in the Gubbio sediments as a function of age. Points are individual values representing the averages of each sample. Arrows indicate data points that are off scale. The shaded band is the 2σ uncertainty on the five-point running mean. $[^4He]_N$ is approximately constant, except between 66 Ma and 68 Ma, where there is a ~threefold increase. See text for discussion. Ages have been computed as in Figure 3.

A collision in the asteroid belt provides a reasonable alternative explanation. Although the temporal variation of dust production following a collision in the asteroid belt has not been modeled in detail, Durda et al. (1992) suggested variations in the dust production rates of asteroid families. In general their model shows large stochastic asymmetric variations in dust production over timescales of millions to tens of millions of years. Thus, the IDP accretion pattern we infer for the late Paleocene to the middle Eocene is consistent with an increase in the dustiness of the inner solar system following a major collision in the asteroid belt. It may also be possible for collisions in the Kuiper belt to produce this increase in IDP accretion. However, this is speculative since the temporal evolution of dust production in the Kuiper belt is even more poorly constrained than in the asteroid belt.

5.1.1. Implications for comet shower periodicity

Several investigators have suggested that showers of long-period comets may recur with a fixed period and may be responsible for mass extinction events (e.g., Alvarez and Muller, 1984; Davis et al., 1984; Rampino and Stothers, 1984a,b). While arguments against periodic cometary impacts have been presented (e.g., Weissman, 1985; Montanari et al., 1998), modulation of the Oort cloud resulting from the vertical oscillation of the solar system about the Galactic midplane (e.g., Matese et al., 1995) apparently remains a viable mechanism for generating cyclical comet showers. The period of this motion is uncertain; Matese et al. (1995) favored a value between 30 to 44 Myr while Stothers (1998) suggested a period of 37 ± 4 Myr.

If showers of long-period comets are periodic, the most probable impact crater candidates in the past 75 Myrs are the Popigai and Chesapeake Bay in the late Eocene, the Chicxulub impact at the K/T boundary or the Manson and Kara impact structures in the Maastrichtian. While the increase in IDP accretion rate during the late Eocene may be the result of a shower of long-period comets, Farley et al. (1998) argued against Galactic tidal forcing as a mechanism for its generation. Similarly, we have presented evidence against comet showers associated with the K/T or the Manson and Kara impacts. Indeed, our data preclude major comet showers in the interval from 74 to 39 Ma. If comet showers are periodic, it is not evident from our proxy record of the IDP accretion rate, and comet showers are not associated with any known impact craters in our time window.

5.2. Implications of Terrestrial [^{4}He]

Along with providing insight to relative sedimentation rates, [^{4}He] in sediments is a useful tracer in its own right (Marcantonio et al., 1998; Patterson et al., 1999). In contrast to ^{3}He, ^{4}He in many deep-sea sediments, including those from the Gubbio

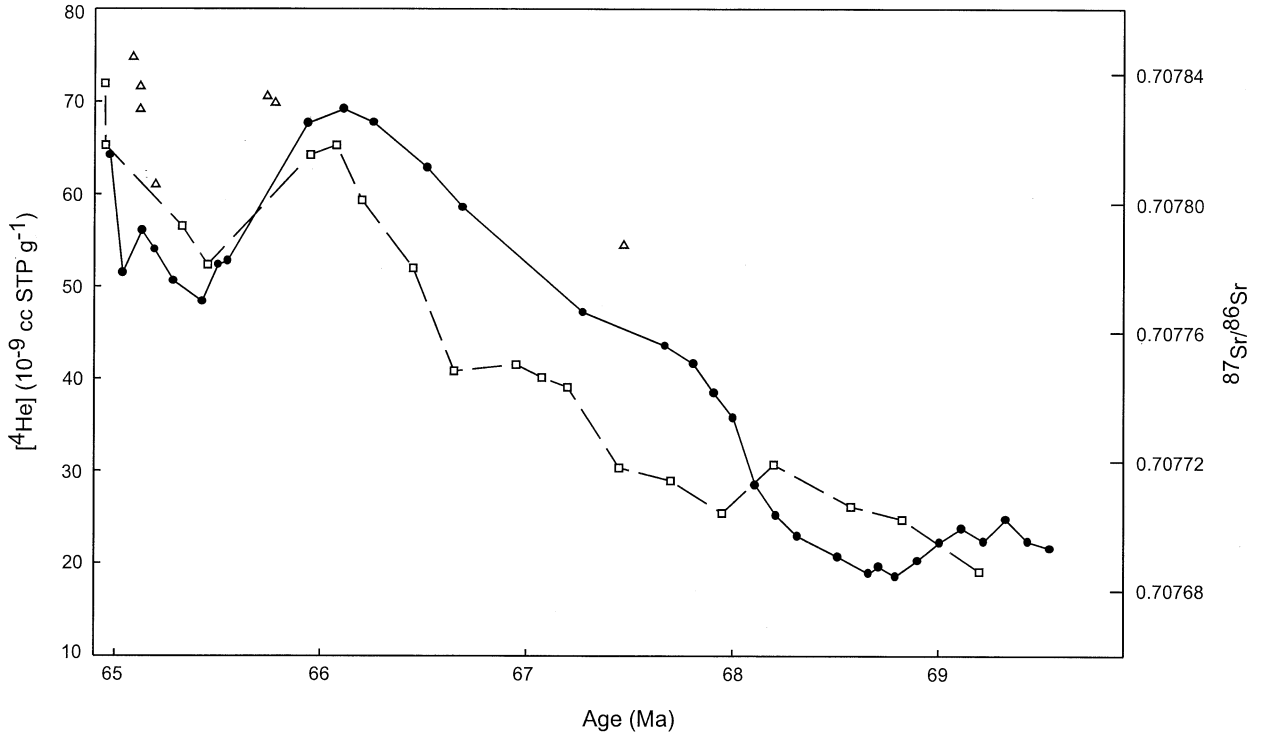

Fig. 7. Seawater Sr-isotopic composition and [^{4}He] as a function of age. Solid circles are [^{4}He] in the Gubbio sediments. Open squares are Sr-isotopic data from Nelson et al. (1991) and open triangles from McArthur et al. (1998).

section, is completely terrestrial in origin. We believe that most of the ^{4}He is transported to the deep sea in a small, He-retentive fraction of the detrital component, possibly zircon (also see Patterson et al., 1999). As shown in Figure 3, there is a strong correlation between ^{4}He and the non-carbonate fraction of the sediment. This is further emphasized in Figure 6, where [^{4}He] is plotted per unit mass of non-carbonate material, ([^{4}He]$_N$). Were [^{4}He]$_N$ constant throughout the record shown in Figure 6, ^{4}He would convey no new information beyond what is available from measurements of the non-carbonate fraction. However, there is a very large increase in [^{4}He]$_N$ in the Maastrichtian (Fig. 6). Before 69 Ma [^{4}He]$_N$ is invariant, but between 69 and 67 Ma it increases threefold, then falls to the nearly constant Cenozoic values. The increase in [^{4}He]$_N$ most likely documents a change in the composition of the terrigenous input, such that starting at approximately 69 Ma there was an influx of geologically older or more U and Th rich crustal material with higher [^{4}He], reaching a maximum just before the K/T boundary.

Figure 7 shows that the increase in [^{4}He]$_N$ correlates well with the Sr-isotope composition of seawater between 68 and 65 Ma, including the maximum at 66 Ma and the rise preceding the K/T boundary. This unexpected correlation provides insights to the mechanism driving the change in seawater strontium and terrigenous He in this interval. The strontium isotope composition of seawater, as recorded by marine carbonates, reflects a globally-averaged balance between radiogenic strontium derived from continental weathering and input of non-radiogenic strontium from midocean ridge hydrothermal activity (e.g., Richter et al., 1992; Jones et al., 1994).

The Late Cretaceous seawater ^{87}Sr/^{86}Sr record was attributed by Jones et al., (1994) to variations in hydrothermal strontium flux. Since [^{4}He] in the terrigenous fraction is not directly affected by hydrothermal activity, changes in hydrothermal activity are not likely to account for the correlation in Figure 7. However it is reasonable to expect that changes in continental weathering modify [^{4}He]$_N$ and ^{87}Sr/^{86}Sr together, for example by shifting the composition of weathered continental material towards more radiogenic Sr and [^{4}He] compositions. Thus our data favor a change in weathering regime or source rocks as an explanation for the [^{4}He]$_N$ and ^{87}Sr/^{86}Sr changes in the last few Myrs of the Cretaceous, and supports the idea of Nelson et al. (1991) of an increased continental strontium flux. It is important to note that the increase in seawater Sr isotopic composition is a global signal, whereas the Gubbio [^{4}He] is a local signal, recording only the detrital components delivered to the Umbria-Marche Basin. If the increased [^{4}He]$_N$ signal is restricted to sediments from this general region, it would imply that climatic/tectonic changes in Southern Europe were the dominant control on the global Sr budget of the oceans in the late Maastrichtian. We are aware of no data with which to evaluate this possibility.

6. SUMMARY AND CONCLUSIONS

We measured the He abundance and isotopic composition of a suite of pelagic limestones exposed in the Italian Apennines that were deposited from ~74 to ~39 Ma. Our data indicate:

- The IDP accretion rate in the Maastrichtian was fairly constant, except for probable but minor increases between ~70.5 Ma and 68 Ma, and at ~66 Ma. These increases are

not likely to be related to showers of long-period comets, but may reflect random events in the asteroid or Kuiper belt

- The IDP accretion rate through the K/T boundary is low and invariant, indicating that the K/T impactor was not a member of a comet shower. Instead, the K/T impactor is more likely to have been a single earth-crossing asteroid or comet.
- We observe a two to fourfold increase in the IDP accretion rate close to the P/E boundary followed by a factor of three decay over a ~4 to 5 Myr period. This increase does not exhibit the temporal pattern expected from a comet shower arising from a gravitational perturbation of the Oort cloud. Instead, our data are more consistent with an increase in IDP accretion resulting from a major collision in the asteroid belt. Collisions in the Kuiper belt may provide an alternate explanation.
- The absence of appropriate peaks in ^{3}He accretion provide strong evidence against long-period comet showers through the 74 to 39 Ma interval. If comet shower periodicity exists, it is either of period longer than 38 Myrs, or the showers do not substantially perturb the ^{3}He accretion rate. The latter seems unlikely given the ^{3}He-based observations for a late Eocene comet shower (Farley et al., 1998).
- The strong correlation between ^{4}He flux and seawater ^{87}Sr/^{86}Sr suggests that the rapid rise in strontium isotopic composition in the three million years before the K/T boundary was, at least in part, driven by a change in the source of continental material delivered to the sea.

Acknowledgments— We thank Kim Robinson, Elizabeth Navarro, and Selene Eltgroth for sample preparation and P. Clayes, B. Peucker-Ehrenbrink, and B. Schmitz for thorough and helpful reviews. This was work was supported by NASA.

Associate editor: C. Koeberl

REFERENCES

Alvarez W. and Muller R. A. (1984) Evidence from crater ages for periodic impacts on the earth. *Nature* **308,** 718–720.

Alvarez W., Asaro F., and Montanari A. (1990) Iridium profile for 10 million years across the Cretaceous-Tertiary boundary at Gubbio (Italy). *Science* **250,** 1700–1702.

Alvarez W., Arthur M., Fischer A., Lowrie W., Napoleone G., Premoli Silva I., and Roggenthen W. (1977) Upper Cretaceous-Paleocene magnetic stratigraphy at Gubbio, Italy. V. Type section for the Late Cretaceous-Paleocene geomagnetic reversal time scale. *Geol. Soc. Am. Bull.* **88,** 367–389.

Andrews J. N. (1985) The isotopic composition of radiogenic helium and its use to study groundwater movement in confined aquifers. *Chem. Geol.* **49,** 339–351.

Andrews J. N. and Kay R. L. F. (1982) Natural production of tritium in permeable rocks. *Nature* **298,** 361–363.

Arthur M. A. and Fischer A. G. (1977) Upper Cretaceous-Paleocene magnetic stratigraphy at Gubbio, Italy. I. Lithostratigraphy and sedimentology. *Geol Soc. Am. Bull.* **88,** 67–371.

Bottomley R. and York D. (1988) Age measurement of the submarine Montagnais impact crater. *Geophys. Res. Lett.* **15,** 1409–1412.

Byl J. (1983) Galactic perturbations on nearly cometary orbits. *Moon and Planets* **29,** 121–137.

Cande S. C. and Kent D. V. (1992) A new geomagnetic polarity time scale for the Late Cretaceous and Cenozoic. *J. Geophys. Res.* **97,** 13917–13951.

Cande S. C. and Kent D. V. (1995) Revised calibration of the geomagnetic polarity timescale for the Late Cretaceous and Cenozoic. *J. Geophy. Res.* **100,** 6093–6095.

Cerling T. and Craig H. (1993) Geomorphology and in-situ cosmogenic isotopes. *Ann. Rev. Earth Planet. Sci.* **22,** 273–317.

Chauris H., LeRousseau J., Beaudoin B., Propson S., and Montanari A. (1998) Inoceramid extinction in the Gubbio basin (northeastern Apennines of Italy) and relations with mid-Maastrichtian environmental change. *Paleogeogr. Paleoclimatol. Paleoecol.* **139,** 177–193.

Clymer A. K., Bice D. M., and Montanari A. (1996) Shocked quartz from the late Eocene: Impact evidence from Massignano, Italy. *Geology* **24,** 483–486.

Davis M., Hut P., and Muller R. (1984) Extinction of species and periodic comet showers. *Nature* **308,** 715–717.

Dermott S. F., Gorgan K., Gustafson B. A. S., Jayaraman S., Kortenkamp S. J., and Xu Y. L. (1996) Sources in interplanetary dust. In *Physics, Chemistry and dynamics of interplanetary dust* (eds. B. A. S. Gustafson and M. S. Hanner) pp. 143–153. Astronom. Soc. Pac. Conf. Ser. Vol. 104.

Durda D. D., Dermott S. F., and Gustafson B. A. S. (1992) Modeling of asteroidal dust production rates. *Asteroids, Comets, Meteors 1991,* (eds. A. W. Harris and E. Bowell), pp. 161–164. Lunar and Planetary Institute, Houston, Texas.

Farley K. A. (1995) Cenozoic variations in the flux of interplanetary dust recorded by ^{3}He in a deep-sea sediment. *Nature* **376,** 153–156.

Farley K. A. (in press). Extraterrestrial helium in seafloor sediments: Identification, characteristics, and accretion rate over geologic time. In *Accretion of Extraterrestrial matter throughout Earth's History* (eds. B. Peucker-Ehrenbrink and B. Schmitz).

Farley K. A. and Patterson D. B. (1995) A 100-kyr periodicity in the flux of extraterrestrial ^{3}He to the sea floor. *Nature* **378,** 600–603.

Farley K. A., Love S. G., and Patterson D. B. (1997) Atmospheric entry heating and helium retentivity of interplanetary dust particles. *Geochim. Cosmochim. Acta* **61,** 2309–2316.

Farley K. A., Montanari A., Shoemaker E. M., and Shoemaker C. S. (1998) Geochemical evidence for a comet shower in the Late Eocene. *Science* **280,** 1250–1252.

Flynn G. J. (1989) Atmospheric entry heating: A criterion to distinguish between asteroidal and cometary sources of interplanetary dust. *Icarus.* **77,** 287–310.

Flynn G. J. (1999) Dust from the Kuiper belt: Modelling the production rate, orbital evolution, and criteria for identification among particles collected at earth. In *Asteroids Comets Meteors.* **1999,** Cornell University, p 30. (abstr.).

Geiss J., Buehler F., Cerutti H., Eberhardt P., and Filleaux C. H. (1972) Solar wind composition experiments. *Apollo 16 Preliminary Sci. Rep.* NASA SP-315, 14.1–14:10.

Gladman B. J. (1997) Dynamical lifetimes of objects injected into asteroid belt resonances. *Science* **277,** 197–201.

Gradstein F. M., Agterberg F. P., Ogg J. G., Hardenbol J., Van Veen P., Thierry J., and Huang Z. (1994) A Mesozoic time scale. *J. Geophys. Res.* **99,** 24051–24074.

Heisler J. and Tremaine S. (1986) The influence of the galactic tidal field on the Oort comet cloud. *Icarus.* **65,** 13–26.

Herbert T. D. and D'Hondt S. L. (1990) Precessional climate cyclicity in Late Cretaceous-Tertiary marine sediments: A high resolution chronometer of Cretaceous-Tertiary boundary events. *Earth Planet. Sci. Lett.* **99,** 263–275.

Hills J. G. (1981) Comet showers and the steady-state infall of comets from the Oort cloud. *Astron. J.* **86,** 1730–1740.

Hiyagon H. (1994) Retention of solar helium and neon in IDPs in deep sea sediments. *Science* **263,** 1257–1259.

Hut P., Alvarez W., Elder W. P., Hansen T., Kauffman E. G., Keller G., Shoemaker E. M., and Weissman P. R. (1987) Comet showers as a cause of mass extinctions. *Nature* **329,** 118–126.

Izett G. A., Cobban W. A., Dalrymple G. B., and Obradovich J. D. (1998) ^{40}Ar/^{39}Ar age of the Manson impact structure, Iowa, and correlative impact ejecta in the Crow Creek Member of the Pierre Shale (Upper Cretaceous), South Dakota and Nebraska. *Geol. Soc. Am. Bull.* **110,** 361–376.

Izett G. A., Masaitis V. L., Shoemaker E. M., Dalrymple G. B., and Steiner M. B. (1994) Eocene age of the Kamensk buried crater of Russia. In *New developments regarding the KT event and other catastrophes in Earth history. LPI Contrib.* **825,** 55–56. (abstr.).

Jones C. E., Jenkyns C. H., Coe A. L., and Hesselbo S. P. (1994) Strontium isotopic variations in Jurassic and Cretaceous seawater. *Geochim. Cosmochim. Acta* **58,** 3061–3074.

Koeberl C., Sharpton V. L., Murali A. V., and Burke K. (1990) Kara and Ust-Kara impact structures (USSR) and their relevance to the K/T boundary event. *Geology* **18,** 50–53.

Kortenkamp S. J. and Dermott S. F. (1998a) Accretion of interplanetary dust particles by the Earth. *Icarus.* **135,** 469–495.
Kortenkamp S. J. and Dermott S. F. (1998b) A 100,000-year periodicity in the accretion rate of interplanetary dust. *Science* **280,** 874–876.
Kyte F. T. (1998) A meteorite from the Cretaceous/Tertiary boundary. *Nature* **396,** 237–239.
Kyte F. T. and Wasson J. T. (1986) Accretion rate of extraterrestrial matter: Iridium deposited 33 to 67 million years ago. *Science* **232,** 1225–1229.
Lal D. (1987) Production of ^{3}He in terrestrial rocks. *Chem. Geol.* **66,** 89–98.
Liou J. C., Dermott S. F., and Xu Y. L. (1995) The contribution of cometary dust to the zodiacal cloud. *Planet. Space Sci.* **43,** 717–722.
Liou J. C., Zook H. A., and Dermott S. F. (1996) Kuiper belt dust grains as a source of interplanetary dust particles. *Icarus.* **124,** 429–440.
Loosli H. H., Lehmann B. E., Gautschi A., and Tolstikhin I. N. (1995) Helium isotopes in rocks, minerals and related groundwaters. In *Water-Rock Interaction* (eds. Y. K. Kharara and O. Chudaev), pp. 31–34. Proc. 8th International Symp. Water-Rock-Interaction, Vladivostok.
Love S. G. and Brownlee D. E. (1993) A direct measurement of the terrestrial mass accretion rate of cosmic dust. *Science* **262,** 550–553.
Lowrie W. and Alvarez W. (1977) Upper Cretaceous-Paleocene magnetic stratigraphy at Gubbio, Italy, III. Upper Cretaceous magnetic stratigraphy. *Geol. Soc. Am. Bull.* **88,** 374–377.
Lowrie W., Alvarez W., Napoleone G., Perch-Nielsen K., Premoli Silva I., and Toumarkine M. (1982) Paleogene magnetic stratigraphy in Umbrian pelagic carbonate rocks: The Contessa sections, Gubbio. *Geol. Soc. Am. Bull.* **93,** 414–432.
Marcantonio F., Anderson R. F., Stute M., Kumar N., Schlosser P., and Mix A. (1996) Extraterrestrial ^{3}He as a tracer of marine sediment transport. *Nature* **383,** 705–707.
Marcantonio F., Higgins S., Anderson R. F., Stute M., Schlosser P., and Rasbury E. T. (1998) Terrigenous helium in deep-sea sediments. *Geochim. Cosmochim. Acta* **62,** 1535–1543.
Matese J. J., Whitman P. G., Innanen K. A., and Valtonen M. J. (1995) Periodic modulation of the Oort Cloud comet flux by the adiabatically changing galactic tide. *Icarus.* **116,** 255–268.
Merrihue C. (1964) Rare gas evidence for cosmic dust in modern Pacific red clay. *Ann. N.Y. Acad. Sci.* **119,** 403–411.
McArthur J. M., Thirlwall M. F., Engkilde M., Zinsmeister W. J., and Howarth R. J. (1998) Strontium isotope profile across the K/T boundary sequences in Denmark and Antartica. *Earth Planet. Sci. Lett.* **160,** 179–192.
McHone J. F. and Sorkhabi R. S. (1994) Apatite fission-track age of Marquez Dome impact structure. *Lunar Planet. Sci.* **XXV,** 881–882. (abstr.).
Monechi S. and Thierstein H. R. (1985) Late Cretaceous-Eocene nannofosil and magnetostratigraphic correlations near Gubbio, Italy. *Mar. Micropaleontology* **9,** 419–440.
Montanari A. and Koeberl C. (2000) Impact stratigraphy: The Italian record. Springer-Verlag, 364 pp.
Montanari A., Bagatin A. C., and Farinella P. (1998) Earth cratering record and impact energy flux in the last 150 Ma. *Planet Space. Sci.* **46,** 271–281.
Montanari A., Asaro F., Michel H. V., and Kennett J. P. (1993) Iridium anomalies of late Eocene age at Massignano (Italy), and ODP site 689B (Maud Rise, Antarctic). *Palaios.* **8,** 420–437.
Mukhopadhyay S., Farley K. A., and Montanari A. (2000) A short duration of the Cretaceous/Tertiary boundary event: Evidence from extraterrestrial ^{3}He. *Science* (submitted).
Napoleone G., Premoli Silva I., Heller F., Cheli P., Corezzi S., and Fischer A. G. (1983) Eocene magnetic stratigraphy at Gubbio, Italy, and its implications for Paleogene geochronology. *Geol. Soc. Am. Bull.* **94,** 181–191.
Nazarov M. A., Badjukov D. D., Barsukova L. D., and Alekseev A. S. (1991) Reconstruction of original morphology of the Kara impact structure and its relevance to the K/T boundary event. *Lunar Planet. Sci.* **XXII,** 959–960 (abstr.).
Nelson B. K., Macleod G. K., and Ward P. K. (1991) Rapid change in strontium isotopic composition of sea-water before the Cretaceous Tertiary boundary. *Nature* **351,** 644–647.
Nier A. O. and Schlutter D. J. (1990) Helium and neon isotopes in stratospheric particles. *Meteoritics* **25,** 263–267.
Ozima M. and Podosek F. A. (1983) Noble gas geochemistry. Cambridge University Press, 367 pp.
Ozima M., Takayanagi M., Zashu S., and Amari S. (1984) High ^{3}He/^{4}He in ocean sediments. *Nature* **311,** 449–451.
Patterson D. B. and Farley K. A. (1998) Extraterrestrial ^{3}He in seafloor sediments: Evidence for correlated 100 kyr periodicity in the accretion rate of interplanetary dust, orbital parameters, and Quaternary climate. *Geochim. Cosmochim. Acta* **62,** 3669–3692.
Patterson D. B., Farley K. A., and Schmitz B. (1998) Preservation of extraterrestrial 3He in 480-Ma-old marine limestones. *Earth Planet. Sci. Lett.* **163,** 315–325.
Patterson D. B., Farley K. A., and Norman M. D. (1999) ^{4}He as a tracer of continental dust: A 1.9 million year record of aeolian flux to the west equatorial Pacific Ocean. *Geochim. Cosmochim. Acta* **63,** 615–625.
Pierrard O., Robin E., Rocchia R., and Montanari A. (1998) Extraterrestrial Ni-rich spinel in upper Eocene sediments from Massignano, Italy. *Geology* **26,** 307–310.
Peucker-Ehrenbrink B. (1996) Accretion of extraterrestrial matter during the last 80 million years and its effect on the marine osmium isotope record. *Geochim. Cosmochim. Acta* **60,** 3187–3196.
Premoli Silva I. (1977) Upper Cretaceous-Paleocene magnetic stratigraphy at Gubbio, Italy. II. *Biostratigraphy. Geol. Soc. Am. Bull.* **88,** 371–374.
Rampino M. R. and Stothers R. B. (1984a) Terrestrial mass extinctions, cometary impacts and the Sun's motion perpendicular to the galactic plane. *Nature* **308,** 709–712.
Rampino M. R. and Stothers R. B. (1984b) Geological rhythms and cometary impacts. *Science* **226,** 1427–1431.
Richter F. M., Rowley D. B., and DePaolo D. J. (1992) Sr isotope evolution of seawater: The role of tectonics. *Earth Planet. Sci. Lett.* **109,** 11–23.
Roggenthen W. M. and Napoleone G. (1977) Upper Cretaceous-Paleocene magnetic stratigraphy at Gubbio, Italy. IV. Upper Maastrichtian-Paleocene magnetic stratigraphy. *Geol. Soc. Am. Bull.* **88,** 378–382.
Schmitz B., Asaro F., Molina E., Monechi S., Salis K. V., and Speijer R. P. (1997) High-resolution iridium δ^{13}C, δ^{18}O, foraminifera and nannofossil profiles across the latest Paleocene benthic extinction event at Zumaya, Spain. *Paleogeogr. Paleoclimatol. Paleoecol.* **133,** 49–68.
Sharpton V. L. and Gibson J. W. Jr. (1990) The Marquez Dome impact structure, Leon County, Texas. *Lunar Planet. Sci.* **XXI,** 1136–1137 (abstr.).
Shukolyukov A. and Lugmair G. W. (1998) Isotopic evidence for the Cretaceous-Tertiary impactor and its type. *Science.* **282,** 927–929.
Stothers R. B. (1998) Galactic disk dark matter; terrestrial impact cratering and the law of large numbers. *Mon. Not. R. Astron. Soc.* **300,** 1098–1104.
Stuart F. M., Harrop P. J., Knott S., and Turner G. (1999) Laser extraction of helium isotopes from Antarctic micrometeorites: Source of He and implications for the flux of extraterrestrial ^{3}He flux to earth. *Geochim. Cosmochim. Acta* **63,** 2653–2665.
Takayanagi M. and Ozima M. (1987) Temporal variation of ^{3}He/^{4}He ratio recorded in deep-sea sediment cores. *J. Geophys. Res.* **92,** 12531–12538.
Ten Kate W. G. and Sprenger A. (1993) Orbital cyclicities above and below the Cretaceous/Paleogene boundary at Zumaya (N Spain), Agost and Relleu (SE Spain). *Sed. Geol.* **87,** 69–101.
Tolstikhin I. N. (1978) Some recent advances in isotope geochemistry of light rare gases. In *Advances in Earth and Planetary Sciences, 3.* (eds E. C. Alexander, Jr. and M. Ozima), pp. 33–62. Japan Scientific Societies Press, Tokyo.
Tolstikhin I. N., Lehmann B. E., Loosli H. H., and Gautschi A. (1996) Helium and argon isotopes in rocks, minerals and related groundwaters: A case study in Northern Switzerland. *Geochim. Cosmochim. Acta* **60,** 1497–1514.
Trieloff M., Deutsch A., and Jessberger E. K. (1998) The age of the Kara impact structure, Russia. *Meteoritics Planet. Sci.* **33,** 361–372.
Weissman P. R. (1982) Dynamical history of the Oort cloud. In *Comets* (eds. L. L. Wilkening). Univ. Arizona Press, 637 pp.
Weissman P. R. (1985) Terrestrial impactors at geological boundary events: comets or asteroids? *Nature* **314,** 517–518.